Faculty of Engineering Technology (CTW)

Sound transmission in turbomachinery flow ducts

Internship at DLR-Berlin

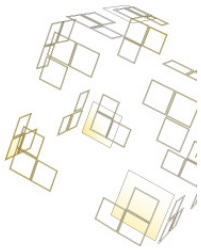

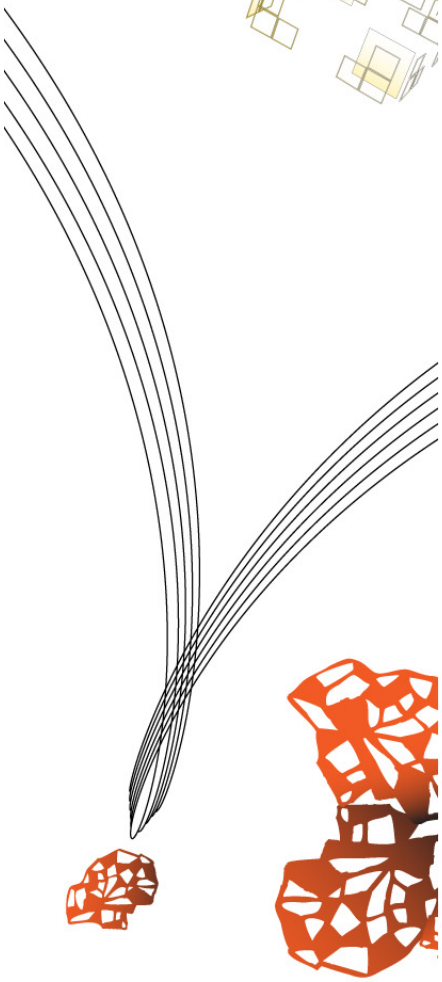

s1005812 Peter Puttkammer

January 15, 2015

Guidance:
U. Tapken *DLR-Berlin*
M. Behn *DLR-Berlin*
Prof. dr. L. Enghardt *DLR-Berlin*
Prof. dr. H.W.M. Hoeijmakers *University of Twente*

UNIVERSITY OF TWENTE.

Contents

Nomenclature

$'$	Term of amplitude without dependency of vorticity
$+$	Upstream propagating wave
$-$	Downstream propagating wave
α_i	Angle of incidence of pressure waves
α_s	Stagger angle
$\alpha_{i,Jenkins}$	Angle of incidence of pressure waves by convention of Jenkins
$\alpha_{i,Kaji}$	Angle of incidence of pressure waves by convention of Kaji and Okazaki
$\bar{v}$	Upwash velocity
$\bar{}$	Reference frame with $\bar{x}$-axis along the blade chord
β	$\sqrt{1-M^2}$
$\breve{}$	Reference frame corresponding to stationary blades and moving duct
$\hat{}$	Amplitude
$\mathcal{P}$	Sound power
$\mathcal{R}$	Reflection coefficient
$\mathcal{T}$	Transmission coefficient
μ	Axial component of the wave number
ν	Gap-wise component of the wave number
Ω	Angular frequency
ω_0	Acoustic frequency
ϕ	Circumferential coordinate
ρ_0	Fluid density
σ	Inter-vane phase difference
$\tilde{}$	Normalized quantities
a	Speed of sound
B	Number of blades

c	Blade chord
I	Power intensity
k	Wave number
M	Mach number
m	Circumferential wave mode order
N	Total number of collocation points
n	Radial wave mode order
p	Pressure perturbation
r	Radial coordinate / integer corresponding to scattering mechanism
R_0	Distance between midpoint of blades and center of duct
s	Blade gap
t	Time
U	Axial component of mean stream velocity
u	Axial component of velocity perturbation
V	Gap-wise component of mean stream velocity
v	Gap-wise component of velocity perturbation
W	Mean stream velocity
x	Axial coordinate
y	Gap-wise coordinate

Chapter 1

Introduction

The main objective of turbomachines is to transfer energy between the rotating impeller blades and the working fluid, in the form of increased/decreased fluid velocity and/or pressure. As a consequence of the change in pressure, pressure waves are formed. These waves propagate through turbomachines, are transmitted and reflected by blade rows and are radiated to the 'far-field' where one experience these waves as noise. The sound intensity radiated from the duct opening may considered to be influenced by the transmission and reflection of the blade rows. Therefore, besides generation of sound, blade rows play an important role in the propagation of sound waves through a turbomachine.

This research is carried out as part of a project (T2.1 *Transmission and Reflection of Blade Rows*) of the German Aerospace Center (*Deutsches Zentrum für Luft- und Raumfahrt*, DLR). The main objectives for this project are:

- Accurate modeling of the propagation of sound through turbomachine stages using analytical methods.
- Development of guidelines for optimizing blade geometries in order to reduce sound transmission through blade row.

The objective of present study is to carry out a literature review with regard to existing analytical models that describe the propagation of sound waves through turbomachinery blade rows. From this literature study, an appropriate model is selected for implementation. The idea is to rewrite the blade row model of Smith [1] such that it can be applied for sound waves propagating through a stator without mean stream flow. It will be seen that the theoretical model is obtained, however the implementation into a calculation program (in this report MATLAB is used) is not (yet) complete.

The literature review regarding existing blade row models is the subject of chapter 2. The general theory for duct acoustics regarding rotors and stators in circular ducts is found in chapter 3. Chapters 4 and 5 discuss the analytical model of Smith. First the original model of Smith - with mean stream flow - is presented, followed by the reformulated model which can be applied for cases without mean stream flow. The first raw results - which are not yet satisfactory - are presented in chapter 6. Finally a conclusion and recommendations are drawn in chapters 7.

Chapter 2

Literature

The present study examines different models for determining the transmission and reflection of sound waves through blade rows. This topic has been subject of multiple studies for the last 40 years, where many developments are achieved. In this section a different blade row models are discussed.

Transmission and reflection of blade rows is first modeled in the beginning of the 1970's. In this period it is identified that the transmission and reflection of pressure waves depend on the incident wave mode. Furthermore concepts such as frequency and mode scattering, although not explicitly mentioned, can be incorporated in the models of the 1970's. From the end of 1990's the computation of a stage (rotor + stator) is investigated, using numerical schemes for coupling different blade rows. Due to the ability of modeling multiple blade rows, other phenomena became of interest such as mode trapping and acoustic resonance. It should be noted that there can be more blade row models found in literature. The selection made in this study is based on the fact that the models specifically discuss the transmission and reflection properties.

2.1 Transmission and reflection of single blade rows

In order to determine the transmission and reflection of sound waves through blade rows, different approaches are investigated by different authors for finding the solution of the equations of compressible flow through a blade row. The methods used vary widely regarding the choice of blade row models and mathematical techniques.

The different models discussed below share a couple of significant assumptions. All blade row models are two-dimensional, but for the blade row model of Glegg [2]. Even Muir [3], who discusses the incidence of three-dimensional waves, uses a two-dimensional semi-actuator disk. Effects of viscosity are neglected and the flow is assumed isentropic. The incoming acoustic waves are plane harmonic waves. Furthermore the blades are unloaded, but Kaji and Okazaki [4] have shown that the effect of blade loading for most incidence angles has little significance.

Kaji and Okazaki (1970) [5] introduced a so-called 'semi-actuator disk' which divided the flow field in three regions: upstream, downstream and within the blades. The semi-actuator disk is a blade row of two-dimensional, flat plates of zero thickness and finite length. However, the blade gap (distance between leading edges of neighboring blades) is infinitesimally small. In this paper only one transmitted and reflected wave are considered. Matching the mass-flux and the pressure at the leading and trailing edges leads to transmission- and reflection coefficients. Muir (1977) [3] generalizes, using an average frequency approach, the semi-actuator disk model to include the incidence of three-dimensional sound waves.

Another possibility for representing a blade row is cascade modeling. In the second part of their paper, Kaji and Okazaki (1970) [4] adopted an approach to incorporate a blade row where

the blade gap is of finite distance. In this approach each blade is represented by an unsteady distribution of pressure doublets which is induced by the incident acoustic pressure wave. In combination with the condition of zero net upwash (normal velocity component) at the blade surface, an integral equation for the unknown doublet distribution function is derived. The solution of the integral equation - which relates the source strength to the velocity and pressure disturbance - is obtained using a collocation procedure, from which the transmitted and reflected noise is determined. Smith (1973) [1] used, instead of pressure doublets, vortices to represent the blades. By doing so, an integral equation for the unknown vorticity distribution along the cascade blades is obtained again using the collocation technique. The change from pressure doublets to vorticity sources is done since it leads to considerable mathematical simplifications.

Mani and Horvay (1970) [6] obtained solutions for the transmission and reflection of blade rows using an approximate solution based on the Wiener-Hopf technique. This technique is used to couple solutions of two partial differential equations with mixed boundary conditions at the same boundary. Mani and Horvay identified two different problems, an incidence and emission problem. The incidence problem covers a plane wave impinging on an infinite set of semi-infinite blades, the emission problem deals with the radiation of the excited blade channel modes by the incident wave at the open ends of a row of semi-infinite blades. These two solutions are combined using the mentioned Wiener-Hopf technique, from which estimates of the transmission and reflection properties of the blade row are derived. Koch (1971) [7] developed the work of Mani and Horvay for blades with finite chord. Koch derives a solution for the reflected and transmitted sound for both upstream and downstream propagating acoustic waves.

Amiet (1971) [8] uses classical isolated flat-plate airfoil theory and the linearized Euler equations to calculate the transmission and reflection of a blade row. In order to do so, Amiet separates the problem into a near- and far-field problem, from which a closed formulation of the problem is stated. Although theoretically this approach can be understood well, the practical implementation seemed rather difficult since it deals with isolated blades rather than a blade row. Therefore this theory it is not used in many blade row models developed after the 1970's in contrast to the models of Kaji and Okazaki, Smith and Koch.

Important parameters that influence the transmission and reflection of sound waves through blade rows is investigated by Kaji and Okazaki [4], and confirmed by others (e.g. [7], [8]). The flow Mach number and the angle of incidence both have great influence on the transmission. For increasing Mach numbers, the transmission coefficient will decrease. Furthermore sound waves hitting the blade row at large angle of incidence can resemble a sound wave hitting a wall, which of course will decrease the transmission coefficient. Kaji and Okazaki also found that the wave length and the steady aerodynamic blade loading both have minor influence on the transmission coefficient.

2.2 Frequency and mode scattering

Although not explicitly mentioned, frequency and mode scattering is incorporated in the blade row models of Kaji and Okazaki [4], Smith [1] and Koch [7]. Furthermore Kaji and Okazaki recognized that the transmission and reflection is influenced by the incoming wave mode. They defined two conditions, a sub- and super-resonant condition. In the sub-resonant condition the transmitted and reflected wave have the same wavelengths as the incoming wave, implying frequency and mode scattering will not occur. For the super-resonant condition also waves with wavelengths different from the incoming wave starts to propagate in up- and downstream direction due to the fact that the waves can be scattered in terms of frequency and mode. Koch and Smith discuss and implement these definitions in their respective papers.

Topol (1987) [9] concretized the transmitted and reflected waves for the super-resonant

condition. To come to this concretization, Topol introduces a model containing one rotor and stator blade row (called a 'stage'), for which a rather simple analytical model is derived which shows that noise modes at blade passing frequency (BPF) can be 'cut-off' (decaying wave modes) in the in- and outlet of the turbomachine, but can be 'cut-on' (propagating wave modes) in the region between the rotor and the stator ('swirl region'). This indicates that BPF mode noise impinging to the stator is partly reflected and propagating upstream towards the rotating rotor blades. Incidence with the rotor blades induces noise which is reflected from the rotor containing partially carried in modes at higher harmonics of BPF that are also cut-on. It is shown that these modes with higher harmonics can dominate the overall noise at specific rotor angular velocities. Comparisons with model fan test, conducted and described in this paper, and full-scale engine data are carried out.

This frequency scattering by rotating rotor blades, described by Topol, is not the only scatter mechanism that needs to be considered. Also modal scattering is an important feature, since it not only takes place at the rotating rotor, but also at the stationary stator. In cylindrical ducts the circumferential mode orders are restricted to the values of m ($m = nB - kV$) [10] resulting from integer values of the rotor n and stator scattering indices k. B is the number of rotor blades, V is the number of stator vanes. Hanson (1993) [11] formulated a model, based on the method of Smith, which includes this mode scattering mechanism for a coupled system of a rotor, a stator and the in- and outlet of a turbomachine. It is stated that the rotor will scatter on the index n, and the stator will scatter on the index k. In 1997 Hanson [12] wrotes a second paper, where the fundamental behavior of the scattering coefficients is examined for a better understanding of the role of blade row transmission and reflection in noise generation. It is shown that the vane/blade ratio significantly influences the transmission and reflection of different wave modes. Furthermore it is shown that rotors tend to scatter up in BPF order where the reflected energy can exceed the incident energy by a substantial amount.

Above mentioned models of Topol and Hanson are valid for tonal noise. However, they do not describe the transmission and reflection of broadband noise. Hanson (2001) [13] adopted the rectilinear cascade model of Glegg (1999) [2] and developed a coupled model for broadband noise. Glegg derived exact analytical expressions for the acoustic field radiated from a three-dimensional blade row, in contrast to the two-dimensional model of Smith. Hanson discovered an analytical approach for tracking broadband noise modes dividing them into what he calls 'independent mode sub-sets'. This makes the broadband problem tractable and it is the basis for the analysis.

Also based on Glegg, Posson (2013) [14] discusses a model for a *"study that aims to develop and assess an analytical model for the sound transmission through an annular stator row in a configuration without mean flow"*. In this study, Glegg's rectilinear model for a single blade row is used to calculate the transmission and reflection of pressure waves (see Posson, Appendix A). Posson extends this model to an annular stator row, from which satisfactory results are found. One should however be aware that the mathematical background of this advanced model is complex, which can make it difficult to understand the physics and the usability of this model.

2.3 Mode trapping and acoustic resonance

Another important contribution of Hanson [11] is the formulation of a generalized coupling scheme, for which isolated elements such as the stator and the rotor can be calculated as one system. When the system is modeled with coupling and swirl included, a phenomenon Hanson calls 'mode trapping' is identified. When a wave mode is trapped between a rotor and stator row it can build up to high levels as it couples to the higher harmonics. These higher harmonics can escape to the in- or outlet, for which it is explained that the noise escaping from the system is at

higher harmonics. So at specific rotor rotating speeds, where mode trapping occurs, the higher harmonics can dominate the overall noise. Topol (1997) [15], employing the additional theory of Hanson, presents an alternative method for a coupled system from which similar results are found. Silkowski (1997) [16] - awarded the Best Paper Award 1997 from the Structures and Dynamics Committee - also derives a coupled mode analysis, extended for blades with camber and thickness.

Additional contribution to the overall noise level that is recently investigated is the topic of acoustic resonance. When traveling pressure waves constructively interfere with each other one speaks of acoustic resonance. This phenomenon can take place between a rotor and stator at specific conditions, which results in a (dominating) contribution to the overall noise levels. Pioneering work on acoustic resonance is studied by Parker and co-workers (e.g. [17]). Hellmich (2008) [18] investigates acoustic resonance in a high-speed axial compressor, using the blade row model of Koch. Hellmich states that acoustic resonance is excited at high rotor speeds with comparably low mass flow only.

2.4 Summary

- The blade row models of Smith and Koch are widely used in literature.
- Frequency scattering occurs only at rotors. Mode scattering occurs at both rotors and stators.
- Coupled numeric schemes are used to carry out calculations on stages instead of isolated blade rows.
- Mode trapping and acoustic resonance should be considered for calculations on coupled blade rows.

Chapter 3

Theoretical expressions for pressure modes

Industrial turbomachines and airplane engines generate sound which radiates through, mostly circular, ducts. These ducts restrict the sound propagation characteristics by corresponding boundary conditions. The study of the propagation of sound waves through ducts is called 'Duct Acoustics' [19]. The equations in this chapter are valid for flows with and without mean flow. If there is mean flow present, it is assumed that this mean stream flow passes through the cascade undeflected.

3.1 Pressure wave in cylindrical duct

The governing equations supporting the theory of duct acoustics are based on the conservation equations of mass, momentum and energy. The propagation of sound - for ducts with various cross-sections and different conditions of flow - has been subject of many studies. By assuming that acoustic fluctuations are small perturbations of pressure, density, velocity and temperature, the linearized conservation equations can be derived. Combining these linearized equations leads to the derivation of the governing wave equations, describing the propagation of sound through a specific duct.

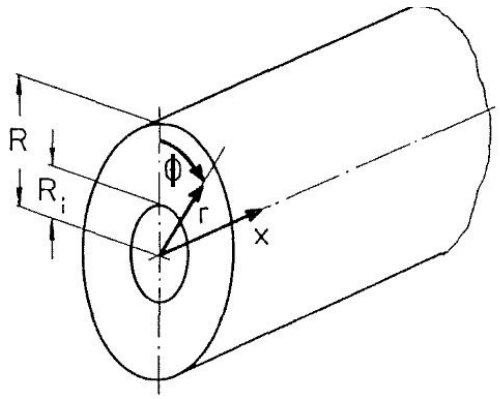

Figure 3.1: cylindrical duct [19]

The wave equation can be solved using the method of separation of variables, where it is assumed that the pressure p is a function of three space coordinates (r, ϕ, z) and time (t). By applying the boundary conditions, the specific representation of the pressure wave through the duct is found. Without applying the boundary conditions, the general solution for the incoming

sound in terms of the pressure reads [19]:

$$p^{\pm}_{n,m}(x,r,\phi,t) = \hat{p}_{n,m} f_{n,m}(r) e^{i(\omega_0 t + \mu^{\pm}_{n,m} x + m\phi)} \tag{3.1}$$

Where $p^{\pm}_{n,m}$ is a pressure wave mode, depending on the spatial and time coordinates and the radial and circumferential wave mode order. Furthermore $\hat{p}_{n,m}$ is the amplitude of the wave mode, $f(r)$ a function - typically expressible in terms of Bessel functions - depending on the radial position r, the acoustic frequency ω_0 and the axial and circumferential wave numbers $\mu^{\pm}_m$ and m. The $\pm$ sign indicates the direction of propagation, '+' is a pressure wave propagating upstream, '−' a wave in downstream direction. One should be aware that this 'plus-minus' sign convention can be used different in literature.

3.2 Pressure wave in unwrapped cylindrical duct

In order to investigate the transmission and reflection characteristics of a blade row, a two-dimensional model is often used in literature. Therefore the three-dimensional wave mode (equation 3.1) should be converted into a two-dimensional wave mode and similar considerations are needed for the blade row.

The cascade model is used to represent the circular blade row. It is necessary to adopt simplifying assumptions since rotor blades and stator vanes have complex geometry (thickness, shape changes, camber, angles). A rotor/stator is divided in so-called annular strips. These strips are unwrapped to form a two-dimensional blade row ('cascade') consisting of flat plates with zero thickness. In figure 3.2 this procedure is displayed.

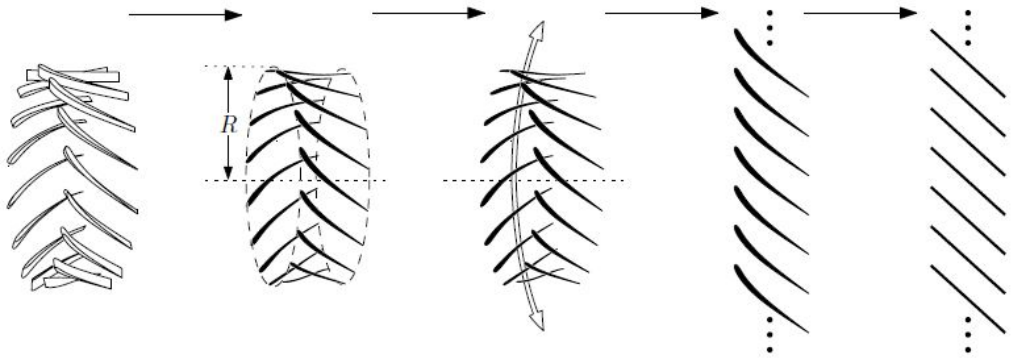

Figure 3.2: Unwrapped cascade model [20]

The incoming sound should be rewritten in terms of this unwrapped cascade model. In order to carry out this procedure, the radial dependency is neglected. This can be assumed since the radial variation of the pressure waves is small compared to the circumferential and axial variation. Topol [15] showed that the influence of radial modes is only significant when rotor/stator interaction is considered at high rotor speeds including mode scattering. So for relations of single rotors or stators this radial dependency can be neglected. A linear coordinate transformation of the circumferential coordinate ϕ is applied by writing it as the gap-wise coordinate divided by the distance between the midpoint of the blades and the center of the circular duct R_0 (see figure 3.3):

$$\phi = \frac{y}{R_0} \tag{3.2}$$

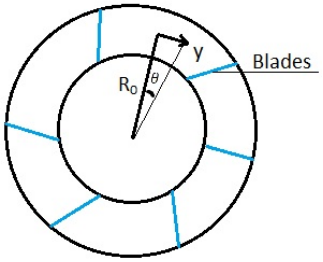

Figure 3.3: Gap-wise coordinate

Then ϕ can be written in terms of the blade gap s and blade number B, since the blade gap can be expressed as:

$$s = \frac{2\pi R_0}{B} \tag{3.3}$$

Combining equations 3.2 and 3.3, the circumferential coordinate ϕ is rewritten as:

$$\phi = \frac{2\pi}{Bs} y \tag{3.4}$$

Substituting this expression into the pressure wave (equation 3.1), neglecting the radial dependency, yields:

$$p_m^{\pm}(x,y,t) = \hat{p}_m e^{i(\omega_0 t + \mu_m^{\pm} x + \nu_m y)} \tag{3.5}$$

$$with: \nu_m = \frac{2\pi m}{Bs} \tag{3.6}$$

This is a pressure wave of circular mode m with still the acoustic frequency ω_o and axial wave number $\mu_m^{\pm}$, but now with the gap-wise wave number ν_m instead of the circumferential wave number m. The axial wave number also is written with a subscript m, indicating that this is also dependent on the circumferential wave number. This dependency can be verified by substituting the pressure mode of equation 3.5 into the convected wave equation for a uniform mean flow and an isentropic medium in the two-dimensional unwrapped coordinate system:

$$\left[\frac{1}{a^2}\left(\frac{\partial}{\partial t} + U\frac{\partial}{\partial x} + V\frac{\partial}{\partial y}\right)^2 - \nabla^2\right] p_m^{\pm}(x,y,t) = 0 \tag{3.7}$$

With a the speed of sound and U and V the mean flow velocity components in axial and gap-wise direction respectively. Carrying out the substitution leads to the dispersion relation for the pressure wave in the unwrapped coordinate system:

$$\left(\frac{\omega_0}{a} + M_x\mu_m^{\pm} + M_y\nu_m\right)^2 - \left((\mu_m^{\pm})^2 + \nu_m^2\right) = 0 \tag{3.8}$$

With the axial flow Mach number M_x $(= \frac{U}{a})$ and the gap-wise flow Mach number M_y $(= \frac{V}{a})$. From this relation the axial wave number can be solved:

$$\mu_m^{\pm} = \frac{M_x\left(\frac{\omega_0}{a} + M_y\nu_m\right) \pm \sqrt{\left(\frac{\omega_0}{a} + M_y\nu_m\right)^2 - \beta_x^2\nu_m^2}}{\beta_x^2} \tag{3.9}$$

With β_x is a short notation for $\sqrt{1-M_x^2}$. Equation 3.9 is a similar relation as found in Smith [1]. This expression indeed shows that the axial wave number is a function of the gap-wise wave number, therefore depending on the circumferential wave number m. Furthermore

this indicates the difference between the so-called 'cut-on' and 'cut-off' wave modes. If $\mu_m^{\pm}$ is real valued, the wave mode is cut-on, which indicates that the pressure waves will propagate up- and downstream. If $\mu_m^{\pm}$ has an imaginary part, the wave modes will decay exponentially and therefore not propagate towards the up- and downstream infinity (cut-off). So the wave mode is cut-on if:

$$\left(\frac{\omega_0}{a} + M_y\nu_m\right)^2 - \beta_x^2\nu_m^2 > 0 \tag{3.10}$$

Summarizing the notation for an incoming pressure wave, created by sound of acoustic frequency ω_0 far up- (-) or downstream (+), applied in the unwrapped two-dimensional reference frame with amplitude $\hat{p}_{inc,m}$ (subscript 'inc' denotes the incoming pressure wave), the axial component x and the gap-wise component y, of circumferential mode order m impinging a blade row of B blades and blade gap s:

$$\begin{aligned} p_{inc,m}^{\pm}(x,y,t) &= \hat{p}_{inc,m} e^{i(\omega_0 t + \mu_{inc,m}^{\pm} x + \nu_{inc,m} y)} \\ with: \nu_{inc,m} &= \frac{2\pi m}{Bs} \\ and: \mu_{inc,m}^{\pm} &= \frac{M_x\left(\frac{\omega_0}{a} + M_y\nu_{inc,m}\right) \pm \sqrt{\left(\frac{\omega_0}{a} + M_y\nu_{inc,m}\right)^2 - \beta_x^2\nu_{inc,m}^2}}{\beta_x^2} \end{aligned} \tag{3.11}$$

3.3 Mode and frequency scattering

Already discussed in the literature chapter, mode and frequency scattering are phenomena occurring with sound waves impinging on rotors and stators. Mode scattering is the mechanism of an incident wave consisting of a single circumferential wave mode m which is reflected and transmitted in pressure waves consisting of multiple wave modes due to the periodic nature of the blade rows. When the blade rows also move (rotors), the frequency of the transmitted and reflected can be shifted into other frequencies, which is called frequency scattering. It will be shown that the scattered modes and frequencies are not random but behave such that this mechanism can be analyzed.

Also discussed in the literature chapter are the sub- and super-resonant conditions. These conditions are first described in the paper of Kaji and Okazaki [4] and they indicate whether or not scattering will occur. In their paper explicit relations are formulated and it can be understood by this simple example. If the gap-wise component of the wavelength is small enough such that at least a half period wave impinges between the leading edges of two blades, the condition is called super-resonant and frequency and mode scattering will occur. If half a period does not fit between the blades, the wavelength is too long compared to the blade gap, the condition is called sub-resonant, and therefore no scattering will occur. Since in this report only the sub-critical regime is investigated, the sub-critical condition is presented. The condition is sub-resonant if the wave number, which is a combination of the axial and gap-wise wave number ($k^2 = \mu^2 + \nu^2$), satisfies:

$$k \leq \frac{\pi}{s}\frac{1 - M^2}{\sqrt{1 - M^2\cos^2\alpha_s}} \tag{3.12}$$

The blade stagger angle is indicated with α_s and it is visualized in figure 3.4.

3.4 Inter-vane phase difference

Consider an incident pressure wave of circumferential mode order m propagating in the right-direction (downstream) in figure 3.4. In this figure only the wave in gap-wise direction is visualized for argument sake. The 'real' pressure waves have next to this gap-wise vibration also an axial vibration, which can be seen in figure 3.5. The angle of the direction of propagation

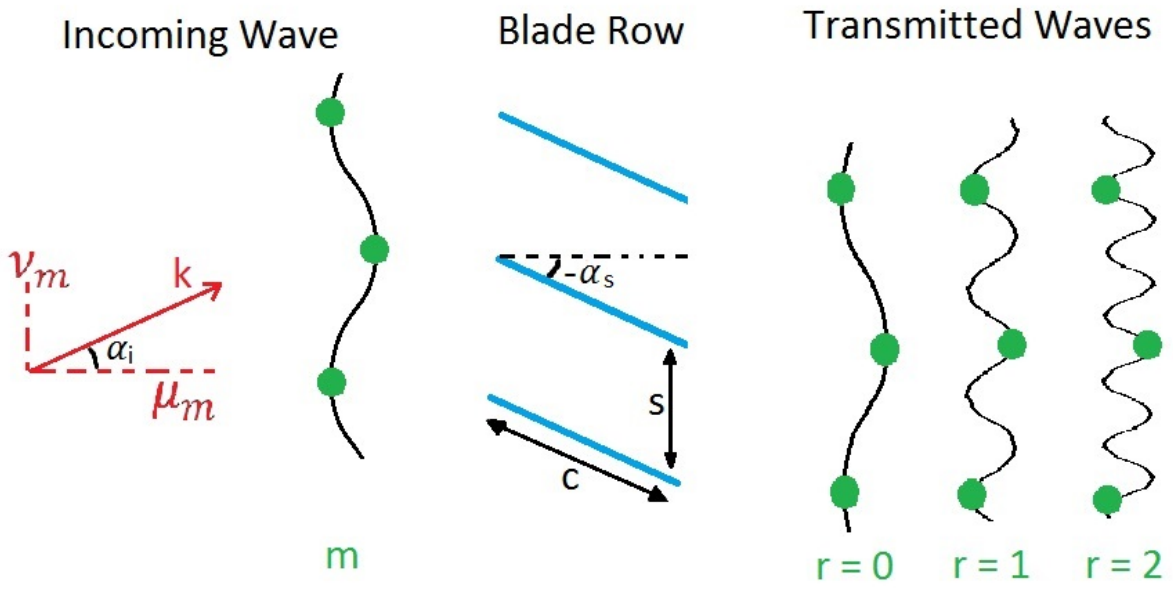

Figure 3.4: Pressure wave impinging on a stator

of the incoming pressure wave is indicated by α_i and the stagger angle by α_s. Due to the periodic nature of the stator, the gap-wise wave number is 'sampled' by the vanes. This is indicated by the inter-vane phase difference, which is in literature also called inter-vane phase angle, inter-blade phase lag angle and more. The inter-vane phase difference indicates the difference of the gap-wise component of the phase of the incoming pressure wave at the leading edge of the blade and its neighbor. If, as displayed in figure 3.5, the incident wave has a non-zero incident angle α_i, the phase of the wave is different at the leading edges of the blades. At the m^{th} blade, the phase of the wave is in general different from the $(m+1)^{th}$ blade.

As will be discussed later, the implementation of the analytic models explained in the next chapters will not yield satisfying results. It is considered that a source of error can be the correct implementation of this inter-vane phase difference, however this is not understand and proven. In the next chapters, the method of Smith [1] will be used to generate a calculation model. Smith and Whitehead [21] (Whiteheads calculation method is used in the model of Smith) do not define the inter-vane phase difference properly. Therefore other sources are consulted which gave - surprisingly - two different definitions. The definitions found are from Kaji and Okazaki [4] and from Jenkins [20]. Both papers use different conventions about the coordinate systems and angles, therefore both are visualized in figure 3.6. Note also that both Kaji and Jenkins use other conventions concerning the angle of incidence of the pressure waves as used in this report. The first definition found in literature is the one from Kaji and Okazaki, here

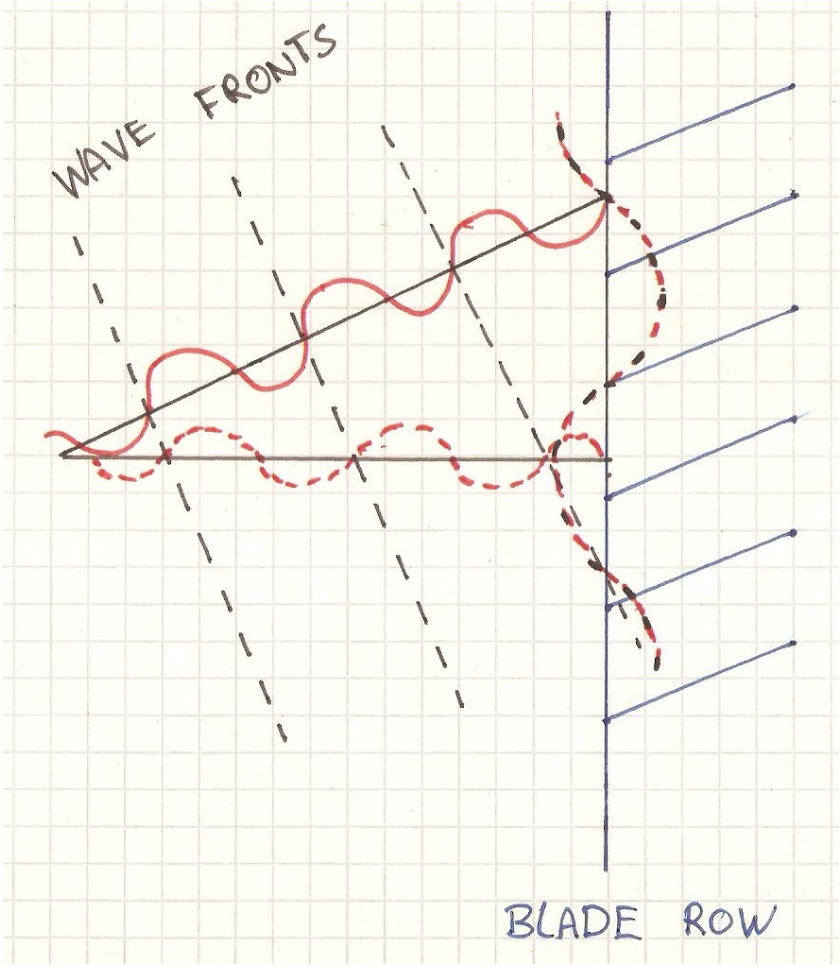

Figure 3.5: Impression of inter-vane phase angle

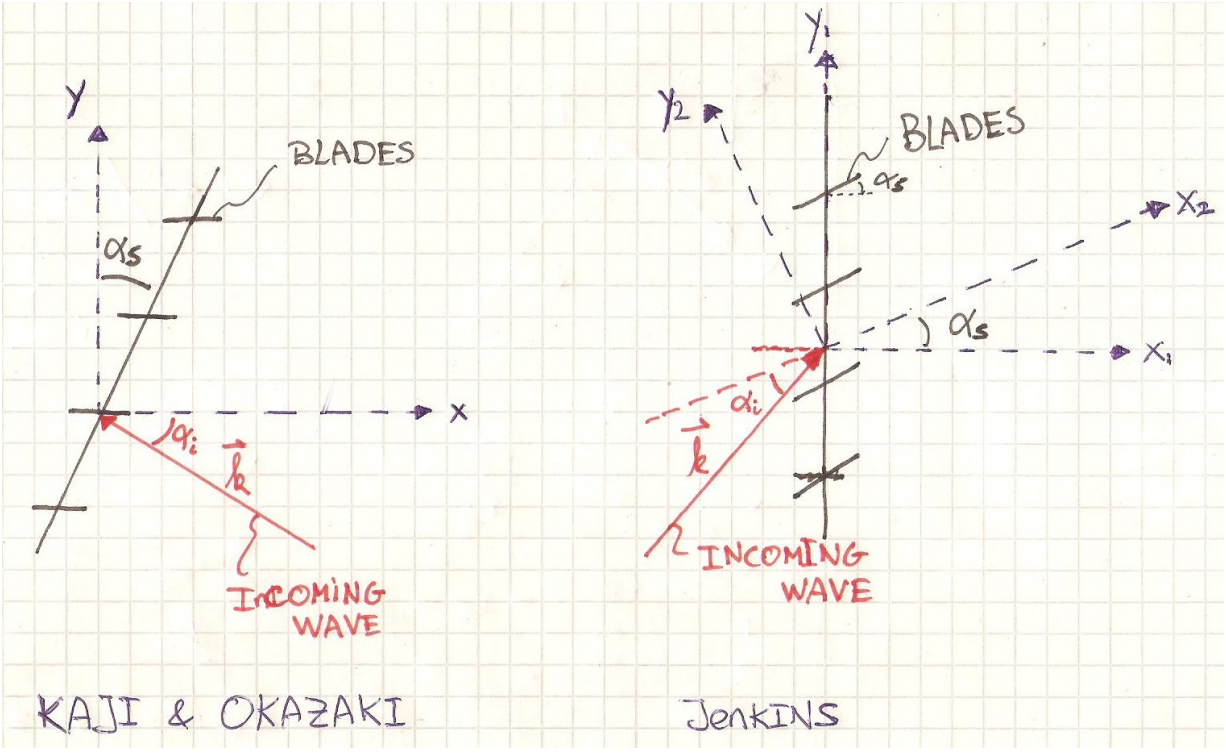

Figure 3.6: Blade row convention of Kaji Okazaki and Jenkins

rewritten using the nomenclature applied in this report:

$$\begin{aligned}\sigma_{Kaji} &= -\frac{ks\sin(\alpha_{i,Kaji}-\alpha_s)}{1-M\cos(\alpha_{i,Kaji})} \\ &= \frac{-1}{1-M\cos(\alpha_{i,Kaji})}ks\left(-\cos(\alpha_{i,Kaji})\sin(\alpha_s)+\sin(\alpha_{i,Kaji})\cos(\alpha_s)\right) \\ &= \frac{-1}{1-M\cos(\alpha_{i,Kaji})}\begin{pmatrix}-k\cos(\alpha_{i,Kaji})\\ k\sin(\alpha_{i,Kaji})\end{pmatrix}\begin{pmatrix}s\sin(\alpha_s)\\ s\cos(\alpha_s)\end{pmatrix}\end{aligned} \tag{3.13}$$

Another definition is found in the report of Jenkins [20], in which is stated that the model of Smith is used:

$$\begin{aligned}\sigma_{Jenkins} &= (k_1\sin(\alpha_s)+k_2\cos(\alpha_s))s \\ &= \begin{pmatrix}k\cos(\alpha_{i,Jenkins})\\ k\sin(\alpha_{i,Jenkins})\end{pmatrix}\begin{pmatrix}s\sin(\alpha_s)\\ s\cos(\alpha_s)\end{pmatrix}\end{aligned} \tag{3.14}$$

With k_1 and k_2 the wave numbers of the incident wave with respect to the chord-aligned coordinate system. As can be seen, although equations 3.13 and 3.14 look similar there are some differences. One can compare the expressions if the incoming wave is similar. This can be achieved if the incoming angle of Kaji is rewritten in terms of the incoming angle of Jenkins:

$$\alpha_{i,Kaji} = \pi - \alpha_{i,Jenkins} \tag{3.15}$$

When this is plugged into equation 3.13, this yields:

$$\sigma_{Kaji} = \frac{-1}{1-M\cos(\alpha_{i,Kaji})}\begin{pmatrix}k\cos(\alpha_{s,Jenkins})\\ k\sin(\alpha_{s,Jenkins})\end{pmatrix}\begin{pmatrix}s\sin(\alpha_s)\\ s\cos(\alpha_s)\end{pmatrix} \tag{3.16}$$

Still two differences between both expressions are observed. For σ_{Kaji} a minus sign is present, whereas in the definition of Jenkins there is not. The second difference is the influence of the velocity of the flow, which is present in the definition of Kaji. It is still unclear what causes these inequalities. Since Jenkins specifically states he uses the model of Smith (Jenkins [20]; first paragraph of "2.3 Pressure radiated from cascade due to velocity perturbation"), it is expected that the definition of Jenkins is the appropriate one.

One last statement can be done for the inter-vane phase difference. If the wave numbers are rewritten in the conventional (x_1,y_1) coordinate system (see convention of Jenkins in figure 3.6, with wave numbers $\mu^{\pm}_{inc,m}$ and $\nu_{inc,m}$, a surprisingly short notation of this phase difference is obtained. The wave number k_1 and k_2 are rewritten following:

$$\begin{aligned}k_1 &= \mu^{\pm}_{inc,m}\cos(\alpha_s)+\nu_{inc,m}\sin(\alpha_s) \\ k_2 &= -\mu^{\pm}_{inc,m}\sin(\alpha_s)+\nu_{inc,m}\cos(\alpha_s)\end{aligned} \tag{3.17}$$

Applying this on equation 3.14, it yields:

$$\sigma_m = \nu_{inc,m}s \tag{3.18}$$

Which is the inter-vane phase difference used in this report.

3.5 Wave modes from stator

The gap-wise wave number of the transmitted (and reflected) sound waves is the summation of the experienced gap-wise wave number (σ_m/s) and the gap-wise wave numbers of waves of the same phase difference:

$$\nu_{m,r} = \frac{\sigma_m + 2\pi r}{s} \tag{3.19}$$

With r is a list of integers $(..,-1,0,1,2,..)$. Applying the definition of the inter-vane phase difference and the gap-wise component of the wave number of the incoming sound wave, this yields:

$$\nu_{m,r} = \frac{2\pi}{Bs}(m + rB) = \frac{2\pi j}{Bs} = \nu_j \tag{3.20}$$

Comparison with equation 3.6 shows that the modal order of j is given by the following scattering rule: $j = m + rB$. Using the dispersion relation (equation 3.9), the corresponding axial wave number for the transmitted and reflected waves by a stator are found. It should be noted that also the strength of the pressure is influenced by the blade row. Or stated differently, the amplitude is altered by the blade row. This influence is investigated and discussed using the method of Smith in the next chapter. Here the transmitted and reflected amplitudes are denoted by $\hat{p}_m^{\pm}$, where '+' still indicates an upstream propagating pressure wave (in this report the reflected wave) and '-' a downstream propagating pressure wave (respectively the transmitted wave). Summarizing the transmitted and reflected pressure wave modes by a stator and the axial and gap-wise wave numbers:

$$\begin{aligned} p_{m,r}^{\pm}(x,y,t) &= \hat{p}_m^{\pm} e^{i(\omega_0 t + \mu_{m,r}^{\pm} x + \nu_{m,r} y)} \\ &with: \nu_{m,r} = \frac{\sigma_m + 2\pi r}{s} \\ &and: \sigma_m = \nu_{inc,m} s \\ &and: \mu_{m,r}^{\pm} = \frac{M_x\left(\frac{\omega_0}{a} + M_y \nu_{m,r}\right) \pm \sqrt{\left(\frac{\omega_0}{a} + M_y \nu_{m,r}\right)^2 - \beta_x^2 \nu_{m,r}^2}}{\beta_x^2} \end{aligned} \tag{3.21}$$

3.6 Wave modes from rotor

Consider a case where the rotor blades rotate in the negative ϕ-direction with angular velocity Ω. In the unwrapped two-dimensional situation, the rotor moves in the negative y-direction with velocity $R_0\Omega$. When moving blades are considered, it is convenient to work with two reference frames. One reference frame (x, y) where the blades are moving and the duct is stationary, and one ($\check{x}$,$\check{y}$) with stationary blades and a moving duct. The reference frames are coupled by:

$$\begin{aligned} \check{x} &= x \\ \check{y} &= y + \Omega \frac{Bs}{2\pi} t \end{aligned} \tag{3.22}$$

The mean velocities are coupled by:

$$\begin{aligned} \check{U} &= U \\ \check{V} &= V + \Omega \frac{Bs}{2\pi} \end{aligned} \tag{3.23}$$

The incident pressure wave of mode m in the fixed-duct reference frame (x, y) is given by equation 3.5. Using the relations between the different reference frames, this incoming wave can be expressed in the fixed-blade reference frame $(\hat{x}, \hat{y})$:

$$\begin{aligned} p^{\pm}_m(x,y,t) &= \hat{p}_{inc,m} e^{i(\omega_0 t + \mu^{\pm}_{inc,m}\check{x} + \nu_{inc,m}(\check{y} - \frac{\Omega B s}{2\pi}t)} \\ &= \hat{p}_{inc,m} e^{i((\omega_0 - m\Omega)t + \mu^{\pm}_{inc,m}\check{x} + \nu_{inc,m}\check{y})} \end{aligned} \tag{3.24}$$

So by shifting between the reference frames, the pressure wave mode is perceived containing a frequency shift:

$$\omega_m = \omega_0 - m\Omega \tag{3.25}$$

In this reference frame with stationary blades, mode scattering can be analyzed similar as for the stator (equation 3.19). When the gap-wise wave number for the transmitted and reflected waves from the rotor are found, the axial wave number can be calculated using the dispersion relation (equation 3.9):

$$\mu^{\pm}_{m,r}(\omega_m) = \frac{\check{M}_x(\frac{\omega_m}{a} + \check{M}_y\nu_{m,r}) \pm \sqrt{(\frac{\omega_m}{a} + \check{M}_y\nu_{m,r})^2 - \check{\beta}^2_x\nu_{m,r}}}{\check{\beta}_x} \tag{3.26}$$

It can be shown that the axial wave number is not influenced by the motion of the blade rows. It is known that $\check{M}_x = M_x$, $\check{M}_y = M_y + \frac{\Omega B s}{2\pi a} = M_y + \frac{\Omega m}{\nu_{inc,m} a}$ and $\check{\beta}_x = \beta_x$. The only term that can contribute to a different axial wave number is:

$$\frac{\omega_m}{a} + \check{M}_y\nu_{inc,m} \tag{3.27}$$

Rewriting this term yields:

$$\frac{\omega_m}{a} + \check{M}_y\nu_{inc,m} = \frac{\omega_m}{a} + M_y\nu_{m,r} + \frac{\Omega m}{a} \tag{3.28}$$

$$= \frac{\omega_m + m\Omega}{a} + M_y\nu_{inc,m} \tag{3.29}$$

$$= \frac{\omega_0}{a} + M_y\nu_{inc,m} \tag{3.30}$$

Which is similar as in the dispersion relation for a stationary duct (equation 3.9). These equalities lead to the observation that the axial wave numbers in the two reference frames are equal:

$$\mu^{\pm}_{m,r}(\omega_m) = \mu^{\pm}_{m,r}(\omega_0) \tag{3.31}$$

So the transmitted and reflected pressure wave modes from a rotor (including change of amplitude: $\hat{p}^{\pm}$). can be written as:

$$p^{\pm}_{m,r}(x,y,t) = \hat{p}^{\pm}_m e^{i(\omega_m t + \mu^{\pm}_{m,r}\check{x} + \nu_{m,r}\check{y})} \tag{3.32}$$

These scattered wave modes can also be written back into the reference frame of the stationary duct using equation 3.22. This procedure yields:

$$p^{\pm}_{m,r}(x,y,t) = \hat{p}^{\pm}_m e^{i(\omega_m t + \mu^{\pm}_{m,r}\check{x} + \nu_{m,r}(y + \Omega\frac{Bs}{2\pi}t)} \tag{3.33}$$

$$= \hat{p}^{\pm}_m e^{i((\omega_m + (\sigma_m + 2\pi r)\frac{\Omega B}{2\pi})t + \mu^{\pm}_{m,r}x + \nu_{m,r}y)} \tag{3.34}$$

In order to understand what is indicated with this transmitted and reflected pressure wave modes, the definition of the inter-vane phase difference is plugged in: $\sigma_m = \nu_{inc,m}s$. Then the frequency term in equation 3.34 can be written as:

$$\omega_m + (\sigma_m + 2\pi r)\frac{\Omega B}{2\pi} = \omega_m + (\nu_{inc,m}s + 2\pi r)\frac{\Omega B}{2\pi} \tag{3.35}$$

Using equation 3.6, the right hand side can be rewritten into:

$$\omega_m + (\frac{2\pi m}{Bs}s + 2\pi r)\frac{\Omega B}{2\pi} = \omega_m + (m + rB)\Omega \tag{3.36}$$

Now substituting the shifted frequency from equation 3.25, which yields:

$$\omega_0 - m\Omega + (m + rB)\Omega = \omega_0 + rB\Omega \tag{3.37}$$

So it is observed that the frequency of the transmitted and reflected waves shift in multiples of the blade passing frequency ($B\Omega$) and therefore moving blades can induce both mode and frequency scattering. The pressure wave mode and the wave numbers for the reflected and transmitted waves from a rotor are summarized below:

$$\begin{aligned} p^{\pm}_{m,r}(x,y,t) &= \hat{p}^{\pm}_m e^{i((\omega_0 + rB\Omega)t + \mu^{\pm}_{m,r}x + \nu_{m,r}y)} \\ with: \nu_{m,r} &= \frac{\sigma_m + 2\pi r}{s} \\ and: \mu^{\pm}_{m,r} &= \frac{M_x\left(\frac{\omega_0}{a} + M_y\nu_{m,r}\right) \pm \sqrt{\left(\frac{\omega_0}{a} + M_y\nu_{m,r}\right)^2 - \beta_x^2\nu_{m,r}^2}}{\beta_x^2} \end{aligned} \tag{3.38}$$

3.7 Transmission and reflection coefficients

In literature transmission and reflection of sound for ducts with stators and rotors is calculated in terms of transmission and reflection coefficients. However one should be aware that these coefficients are not uniquely defined. One definition is the ratio of the pressure amplitudes of the transmitted or reflected wave and the incoming wave, for example used in Smith [1]. Since the pressure amplitudes can be complex valued, the transmission and reflection coefficients are defined as:

$$\begin{aligned} \mathcal{T}_{m,r} &= \frac{\left|\hat{p}^{-}_{m,r}\right|}{\hat{p}_{m,inc}} \\ \mathcal{R}_{m,r} &= \frac{\left|\hat{p}^{+}_{m,r}\right|}{\hat{p}_{m,inc}} \end{aligned} \tag{3.39}$$

Note that it is here assumed that the incoming pressure wave is propagating in downstream (-) direction. Since the method of Smith will be applied in the next chapters, this definition of the transmission and reflection coefficients is used in this report. However, when carrying out more research on different blade row models, the other common used definition of the transmission and reflection coefficients can be applied to examine the validity of these blade row models. This other definition is based on the ratio of the acoustic powers of the transmitted, reflected and incoming sound waves, for example used in Hanson [11], [12]. Since it is known that the energy is a conserved quantity, this definition of the transmission coefficient can give more insight on the model. This was also the idea for this report, however - as will be seen in the next chapters - the calculation models are not yet operational. In Appendix A the transmission and reflection coefficients based on the power ratios for situations without mean stream flow is presented, which can be used in future research.

Chapter 4

Blade row model of Smith with mean stream flow

In this chapter the blade row model of Smith [1] is discussed. The selection for this specific model is based on a couple of arguments. First the model of Smith is supposed to be understood well and a theoretical modification of the model (as carried out in the next chapter) which is valid for cases without mean stream flows seems feasible. Second the model of Hanson [11], [12] yields interesting results regarding the transmission of sound waves through multiple blade rows, in which Hanson applies the blade row model of Smith. Third the model of Koch is used by other departments of DLR. Therefore it is from a scientific perspective interesting to investigate the model of Smith to examine the similarities and differences between both models.

As indicated in the introduction, the idea is to formulate a model for acoustic waves in a circular duct impinging on a stator without mean stream flow. The blade row model of Smith however is only applicable for cases with mean stream flow. Therefore in the next chapter, the model of Smith is rewritten for cases without mean stream flow. It will be showed that the modification of the model changes the governing equations and that it is not possible to set the Mach number simply to zero in the original model of Smith. In this chapter the blade row model of Smith is explained, using references to the original paper of Smith. When it is refered to an equation of Smith, it is written as "equation (S'number')". It should also be noted that the equations from the paper of Smith are here written with the nomenclature used in this report.

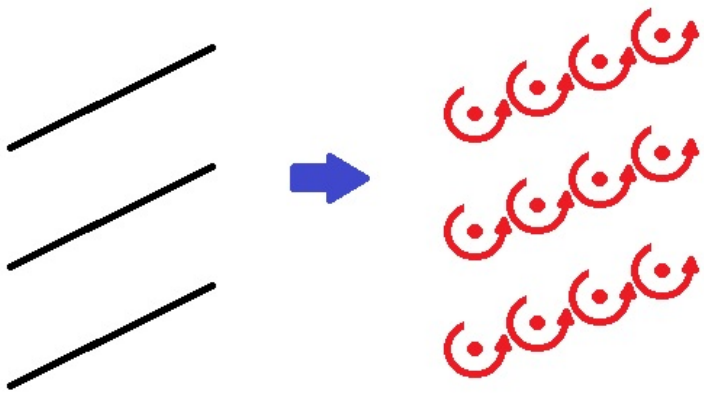

Figure 4.1: Blade model of Smith

4.1 Principle concept

Consider a pressure wave of a single circumferential wave number m originating far upstream with mean flow W impinging on a stator. Note however that the theory discussed in this chapter is also suitable for sound waves impinging on a rotor. It is assumed that the sub-resonant condition is satisfied ($k \leq \frac{\pi}{s}\frac{1-M^2}{\sqrt{1-M^2\cos^2\alpha_s}}$), indicating there will be no mode scattering ($r = 0$ in equation 3.21). Be aware however that, as will be discussed, $r = 0$ cannot simply be applied everywhere in the calculation method of Smith.

Smith argues that a blade row can be represented by multiple vortices placed on the blade surfaces, as visualized in figure 4.1. The principle idea of Smith's method is the following. The incoming acoustic wave incident upon the cascade induces a corresponding upwash velocity distribution on the blades. The upwash velocity is the normal velocity component of the pressure perturbations with respect to the blades. Furthermore the vortices placed on the blades also induce an upwash velocity. Since no air can flow through the blades, the sum of the upwash velocities induced by the incoming pressure wave and by the vortices on the blades should be equal to zero. The vorticity distribution is calculated using the so-called upwash integral equation, which couples the upwash velocities of the incoming pressure wave and of the vortices. The vorticity distribution is then linked directly to the magnitudes of the transmitted and reflected pressure waves, which are used to calculate the transmission and reflection coefficients.

4.2 Governing Equations

Smith starts his paper by making a couple of assumptions. The unwrapped cylindrical duct with flat plates of negligible thickness (figure 3.1) is used in Smith and the mean stream flow passes through the cascade undeflected (mean angle of incidence is zero). Furthermore it is assumed that the waves (two velocity components (u and v) and one pressure component (p)) are plane waves:

$$\begin{aligned} u^{\pm}_{m,r} &= \hat{u}^{\pm}_{m,r}\, {}^{i(\omega_0 t+\mu^{\pm}_{m,r}x+\nu_{m,r}y)} \\ v^{\pm}_{m,r} &= \hat{v}^{\pm}_{m,r} e^{i(\omega_0 t+\mu^{\pm}_{m,r}x+\nu_{m,r}y)} \\ p^{\pm}_{m,r} &= \hat{p}^{\pm}_{m,r} e^{i(\omega_0 t+\mu^{\pm}_{m,r}x+\nu_{m,r}y)} \end{aligned} \tag{4.1}$$

From the linearized equations of continuity and momentum, by assuming the flow is isentropic and the perturbations are indeed plane waves, Smith obtains the characteristic equation (indicating non-trivial solutions of the conservation equations) (equation (S6)):

$$\left[\omega_0 + U\mu^{\pm}_{m,r} + V\nu_{m,r}\right]\left[(\omega_0 + U\mu^{\pm}_{m,r} + V\nu_{m,r})^2 - a^2((\mu^{\pm}_{m,r})^2 + \nu^2_{m,r})\right] = 0 \tag{4.2}$$

From this equation Smith argues that two different physical phenomena are embodied; the term between the first square brackets describe vorticity waves, between the second square brackets pressure waves. This indicates that although only acoustic waves hit the blade row, both pressure waves and vorticity waves, each with different characteristics, need to be considered for the evaluation of the transmitted and reflected waves. Or stated different, the incoming pressure wave is not transmitted (or reflected) in pressure waves only, also part of the incoming wave propagates - after hitting the blade row - in the form of a non-acoustic vorticity wave. The characteristics of the pressure and vorticity waves are found using the definition of the vorticity in the flow and the conservation equations. These characteristics are important, since they yield ratios between the amplitudes of the velocity and pressure components and therefore

are used in Smith's paper to calculate the magnitudes of the far field acoustic waves. These ratios, given in equation (S9) and (S10), are presented here also:

$$\frac{\hat{p}^{\pm}_{m,r}}{\hat{v}^{\pm}_{m,r}} = -\frac{(\omega_0 + U\mu^{\pm}_{m,r} + V\nu_{m,r})\rho_0}{\nu_{m,r}} \tag{4.3}$$

$$\frac{\hat{u}^{\pm}_{m,r}}{\hat{v}^{\pm}_{m,r}} = \frac{\mu^{\pm}_{m,r}}{\nu_{m,r}} \tag{4.4}$$

4.3 Incoming pressure wave

In the paper of Smith, five types of input perturbations are considered. In this report only acoustic waves are of interest. Upstream and downstream propagating acoustic wave incident upon the cascade are stated in Smith. For a downstream propagating acoustic wave, equation (S36) reads:

$$\bar{v}^{-}_{inc,m}(\bar{x}) = -\hat{\bar{v}}_m e^{ic(\mu^{-}_{inc,m}\cos(\alpha_s)+\nu_{inc,m}\sin(\alpha_s))\bar{x}} \tag{4.5}$$

With c the blade chord. It is shown here how to obtain the input perturbations for arbitrary incoming sound waves. From figure 4.2 it can be seen that the upwash velocity corresponding to

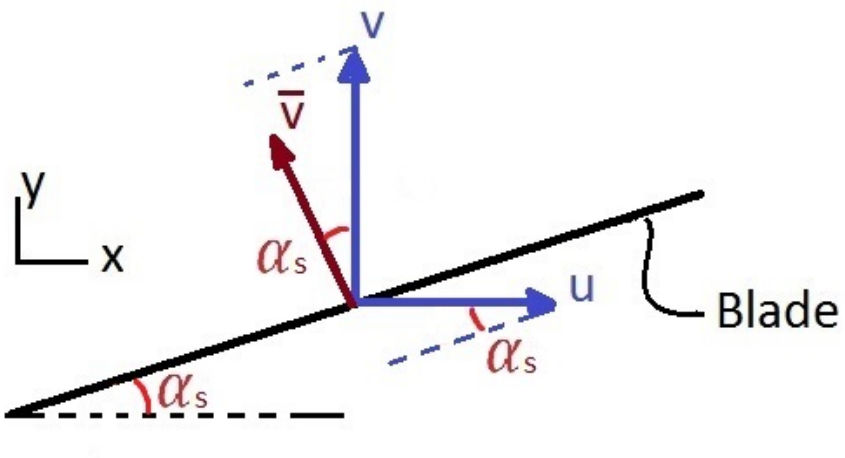

Figure 4.2: Upwash velocity

the blade $\bar{v}$ is a combination of the axial and gap-wise velocity components in the unwrapped two-dimensional reference frame. The upwash velocity for any incoming acoustic wave and arbitrary blade stagger angle can be represented by:

$$\bar{v}^{\pm}_{inc,m} = -u^{\pm}_{inc,m}\sin(\alpha_s) + v_{inc,m}\cos(\alpha_s) \tag{4.6}$$

Using equation 4.3 the upwash velocity can be written in terms of the incoming pressure amplitude:

$$\bar{v}^{\pm}_{inc,m} = \frac{\mu^{\pm}_{inc,m}\sin(\alpha_s) - \nu_{inc,m}\cos(\alpha_s)}{(\omega_0 + U\mu^{\pm}_{inc,m} + V\nu_{inc,m})\rho_0}\hat{p}_{inc,m}e^{i(\omega_0 t+\mu^{\pm}_{inc,m}x+\nu_{inc,m}y)} \tag{4.7}$$

Since the upwash integral equation is written in a reference frame with the $\bar{x}$-axis along the blade chord and $\bar{y}$-axis normal to the blade chord, it is convenient to rewrite the incoming upwash velocity also in this reference frame. This transformation is carried out by:

$$\begin{aligned} x &= \bar{x}\cos(\alpha_s) - \bar{y}\sin(\alpha_s) \\ y &= \bar{x}\sin(\alpha_s) + \bar{y}\cos(\alpha_s) \end{aligned} \tag{4.8}$$

Applying this transformation yields the following expression for the upwash velocity for an arbitrary incoming pressure wave:

$$\bar{v}^{\pm}_{inc,m} = \frac{\mu^{\pm}_{inc,m}\sin(\alpha_s) - \nu_{inc,m}\cos(\alpha_s)}{(\omega_0 + U\mu^{\pm}_{inc,m} + V\nu_{inc,m})\rho_0} \hat{p}_{inc,m} e^{i(\omega_0 t + (\mu^{\pm}_{inc,m}\cos(\alpha_s) + \nu_{inc,m}\sin(\alpha_s))\bar{x} + (-\mu^{\pm}_{inc,m}\sin(\alpha_s) + \nu_{inc,m}\cos(\alpha_s))\bar{y})} \tag{4.9}$$

Which can be written more compact using:

$$\begin{aligned} \bar{\mu}^{\pm}_{m} &= \mu^{\pm}_{m}\cos(\alpha_s) + \nu_m \sin(\alpha_s) \\ \bar{\nu}^{\pm}_{m} &= -\mu^{\pm}_{m}\sin(\alpha_s) + \nu_m \cos(\alpha_s) \end{aligned} \tag{4.10}$$

With this notation, equation 4.9 is written the following:

$$\bar{v}^{\pm}_{inc,m} = -\frac{\bar{\nu}^{\pm}_{inc,m}}{(\omega_0 + U\mu^{\pm}_{inc,m} + V\nu_{inc,m})\rho_0} \hat{p}_{inc,m} e^{i(\omega_0 t + \bar{\mu}^{\pm}_{inc,m}\bar{x} + \bar{\nu}_{inc,m}\bar{y})} \tag{4.11}$$

An assumption for Smith's model is that events occurring at any particular blade are duplicated at all other blades, with a constant phase angle between each blade and its neighbor. This indicates that the analysis can be carried out on a reference blade, placed on the $\bar{x}$-axis. Therefore $\bar{y} = 0$, yielding the upwash velocity for an arbitrary downstream propagating incoming pressure wave for this reference blade:

$$\bar{v}^{-}_{inc,m} = -\frac{\bar{\nu}^{-}_{inc,m}}{(\omega_0 + U\mu^{-}_{inc,m} + V\nu_{inc,m})\rho_0} \hat{p}_{inc,m} e^{i\left(\omega_0 t + \bar{\mu}^{-}_{inc,m}\bar{x}\right)} \tag{4.12}$$

Which has indeed the similar appearance as equation 4.5, only now the amplitude is in terms of known and defined quantities.

4.4 Solution for one vortex row

As already indicated, the condition that there is no net upwash at the blade surface should be satisfied (since no air can flow through the blades). Smith derives relations between the unknown vorticity distribution and a given input velocity perturbation ($\bar{v}^{-}_{inc,m}$) ***and*** between the vorticity distribution and the transmitted and reflected acoustic waves. The vorticity distribution is solved using the relation with the input velocity perturbation ('upwash integral equation'), from which the result is used to determine the magnitudes corresponding to the transmitted and reflected acoustic waves.

First step - in order to calculate the transmitted and reflected acoustic waves - is to examine the conditions to be satisfied by the velocity perturbations produced by the vortices placed on the blades. These vortices form multiple vortex rows (row in gap-wise direction, with blade gap s between two vortices) which fluctuate in strength with amplitude Γ and angular frequency ω_0, with a constant phase angle (inter-vane phase angle) σ_m between each vortex and its direct neighbour on the next blade. The only mention in Smith of the phase angle is done in "2.1 Flow model", where it is stated that the phase angle is an integral fraction of 2π. It is unclear if Smith uses the definition of Kaji and Okazaki [4] or a definition similar to that of Jenkins [20], which is discussed in the previous chapter. Here it is assumed that the definition of the inter-vane phase angle is similar as the definition in Jenkins, since the gap-wise wave number of Smith (equation (S18)) and of Jenkins (Jenkins equation (5.8) are similar and Jenkins states that his approach is based on the method of Smith.

From the conditions - which need to be satisfied by the vorticity distribution - the relation between the vorticity strength and the magnitudes of the transmitted and reflected acoustic waves is found. These boundary conditions are: 1) the equation of continuity through the blade row should be satisfied, 2) the velocity jump in y-direction as the cascade is crossed must be equal to the strength of the vortices on the reference blade (Γ) and 3) a relation between the vorticity in the flow and the strength of the vorticity of the bound vortices placed on the blades must be satisfied. The total effect of the complete vortex row is presented in Smith (equation (S25)), where the amplitude components are given in equations (S23) and (S24)) and here in equation 4.13 and 4.14. The amplitude components are three different expressions, two for the pressure waves $\hat{v}^{\pm}_{m,r}$ and one for the vorticity waves $\hat{v}_{m,r,vortex}$.

$$\hat{v}^{\pm}_{m,r} = \frac{\Gamma}{s}\frac{\nu_{m,r}c}{2A}\left(\mp 1 \mp \frac{\left(\frac{\omega_0 c}{W}\right)}{\nu_{m,r}c}\sin\alpha_s + \frac{i\left(\frac{\omega_0 c}{W}\right)\cos(\alpha_s)}{\sqrt{(\nu_{m,r}c)^2 - M^2 A}}\right) \tag{4.13}$$

$$\hat{v}_{m,r,vortex} = \frac{\Gamma}{s}\frac{\left(\frac{\omega_0 c}{W}\right)^2 + \nu_{m,r}c\left(\frac{\omega_0 c}{W}\right)\sin(\alpha_s)}{A} \tag{4.14}$$

With:

$$\begin{aligned} W &= \sqrt{U^2 + V^2} \\ A &= \left(\frac{\omega_0 c}{W}\right)^2 + (\nu_{m,r}c)^2 + 2\left(\frac{\omega_0 c}{W}\right)\nu_{m,r}c\sin(\alpha_s) \end{aligned} \tag{4.15}$$

An important observation needs to be discussed here concerning equation (S23). In the paper of Smith, the first and third term inside the brackets are dimensionless. However, the second term has the dimension of m^{-1}. It is expected that the gap-wise wave number (in Smith β) should be normalized by multiplying it with the chord length c (in Smith $\hat{\beta}$), such that the second term between brackets dimensionless. This normalization is applied in this report.

Although for the far field acoustic waves only a specific part of pressure modes are present (other modes are cut-off, these modes decay exponentially), all modes effect the near field (since these modes are not decayed immediately). Therefore in order to calculate the upwash velocity perturbations induced by the bounded vortices placed on the blades, all pressure modes ($r = -\infty ... \infty$) need to be considered in the calculation. In terms of the reference frame along the chord ($\bar{x}, \bar{y}$) and applied on the reference blade ($\bar{y}$=0) this reads:

$$\bar{v}^{\pm}_{m,r} = \sum_{r=-\infty}^{\infty} \hat{v}^{\pm}_{m,r} e^{i(\omega_0 t + \bar{\mu}^{\pm}_{m,r}\bar{x})} \tag{4.16}$$

With the amplitude components for pressure perturbations $\hat{v}^{\pm}_{m,r}$ or $\hat{v}_{m,r,vortex}$ for vorticity waves. The dependency of the vorticity strength is implied in these amplitude terms. It should be noted that this equation describes the contribution of one vortex row of the cascade. In the next part the complete blade row, containing multiple vortex rows, is considered.

4.5 Upwash integral equation

When the complete blade row is considered, it should be noted that each chordal element $d\bar{x}$ (with the $\bar{x}$-axis along the blades) of the cascade forms a vortex row. The total upwash induced by the cascade is found by integration along the blade chord, such that the solution is found not for one vortex row, but for all vortex rows along the blades. If one carries out integration along the chord for equation 4.16 and follows the steps in Smith ("2.6 Derivation of Upwash

Integral Equation for cascade"), one finds the upwash integral equation (equation (S30)):

$$\bar{v}^{\pm}_{m,r}(\tilde{x}) = \int_0^1 \gamma(\tilde{x}_0) K(\tilde{x} - \tilde{x}_0) d\tilde{x}_0 \tag{4.17}$$

With γ the vorticity strength density and K the so-called Kernel function, defined in equation (S31) and $\tilde{x} = \frac{1}{c}\bar{x}$. Applying this coordinate transformation also for the upwash velocity for the incoming pressure wave applied on the reference blade (equation 4.12) gives:

$$\bar{v}^{-}_{inc,m}(\tilde{x}) = -\frac{\bar{\nu}^{-}_{inc,m}}{(\omega_0 + U\mu^{-}_{inc,m} + V\nu_{inc,m})\rho_0} \hat{p}_{inc,m} e^{i\left(\omega_0 t + c\hat{\mu}^{-}_{inc,m}\tilde{x}\right)} \tag{4.18}$$

As stated before: The upwash integral equation (equation 4.17) containing the unknown vorticity distribution γ can be solved for an arbitrary input velocity distribution ($\bar{v}^{-}_{inc,m}$) (equation 4.18). This is carried out using a numerical method referred to as a collocation technique. The equation that needs to be evaluated - since zero net upwash at the blades should be satisfied - is:

$$-\bar{v}^{-}_{inc,m}(\tilde{x}) = \int_0^1 \gamma(\tilde{x}_0) K(\tilde{x} - \tilde{x}_0) d\tilde{x}_0 \tag{4.19}$$

So the term on the left hand side of the upwash integral equation describes the upwash velocity of the incoming wave and the integral on the right hand side is the upwash velocity due to the bound vortices placed on the blades.

4.6 Far field acoustic waves

When the vorticity distribution is known by solving the upwash integral equation, the magnitudes of the far field transmitted and reflected acoustic waves ($r = 0$) can be obtained. The dependency of the vorticity distribution on the pressure amplitudes is indicated by equation 4.13, where the gap-wise velocity component can be rewritten into pressure component following equation 4.3. Similar as for the upwash integral equation it should also here be noted that each chordal element of the cascade forms a vortex row which contributes to the magnitudes of the transmitted and reflected waves. This procedure, which is indeed similar as the derivation of the upwash integral equation, leads to the total amplitude of the pressure waves (equation (S39)):

$$\hat{p}^{\pm}_m = -\frac{\rho_0 W}{s/c}(v')^{\pm} \frac{\left(\frac{\omega_0 c}{W}\right) + \mu^{\pm}_m c\cos(\alpha_s) + \nu_m c\sin(\alpha_s)}{\nu_m c} \int_0^1 \gamma(\tilde{x}_0) e^{-ic(\mu^{\pm}_m \cos(\alpha_s) + \nu_m \sin(\alpha_s))\tilde{x}_0} d\tilde{x}_0 \tag{4.20}$$

With v' is the amplitude term of the gap-wise velocity perturbations (equation 4.13) divided by Γ/s. Or stated differently, this is the amplitude term without the dependency of the vorticity strength. Inside the exponent in equation (S39) the imaginary number i is only applied on the term $\mu^{\pm}_m \cos(\alpha_s)$ and not on the second term inside the brackets. It is expected that this is a mistake in Smith's paper, therefore this number i is now written outside of the brackets such that is applied on both terms inside these brackets.

4.7 Numerical evaluation upwash integral equation

In order to evaluate the upwash integral equation, another coordinate transformation is convenient to carry out. Here a transformation to new independent variables ψ and ε, similar as in

a usual thin airfoil theory for single airfoils [21]:

$$\begin{aligned} \tilde{x}_0 &= \frac{1-\cos(\psi)}{2} \\ \tilde{x} &= \frac{1-\cos(\varepsilon)}{2} \end{aligned} \tag{4.21}$$

These new variables are substituted into the upwash integral equation (equation 4.19). The interval boundary will change by:

$$\bar{x}_0 = 1\, then\, 1 = \frac{1-\cos(\psi)}{2} \tag{4.22}$$

$$yielding : \psi = \pi \tag{4.23}$$

The kernel equation will be transformed as follows:

$$K(\tilde{x}-\tilde{x}_0) = K\left(\frac{1-\cos(\varepsilon)}{2} - \frac{1-\cos(\psi)}{2}\right) \tag{4.24}$$

$$= K\left(\frac{\cos(\psi)-\cos(\varepsilon)}{2}\right) \tag{4.25}$$

And $d\tilde{x}_0$ is transformed by:

$$\frac{d\tilde{x}_0}{d\psi} = \frac{\sin(\psi)}{2} \tag{4.26}$$

$$yielding : d\tilde{x}_0 = \frac{\sin(\psi)}{2} d\psi \tag{4.27}$$

Substituting all into the upwash integral equation yields:

$$-\bar{v}^{-}_{inc,m}\left(\frac{1-\cos(\varepsilon)}{2}\right) = \int_0^{\pi} \gamma\left(\frac{1-\cos(\psi)}{2}\right) K\left(\frac{\cos(\psi)-\cos(\varepsilon)}{2}\right)\frac{\sin(\psi)}{2} d\psi \tag{4.28}$$

Next step - in order to evaluate the integral - is to discretize the equation. The bound vorticity can be specified at $(N+1)$ points on a uniform spaced grid, given by:

$$\psi = \frac{\pi l_0}{N} \;\; with : l_0 = 0, 1, 2, ..., N \tag{4.29}$$

The value of γ at the trailing edge ($l_0 = N$) is irrelevant since in equation 4.28 it is always multiplied by $\sin(\psi)$ which is zero for $l_0 = N$. However, this argument does not hold for the leading edge. When solving the upwash integral equation, the vorticity strength γ per unit length will become infinite at the leading edge ($l_0 = 0$). This is also obtained in two-dimensional thin airfoil theory where the Biot-Savart law is used in combination with Glauert's approximation (see Anderson [22]) of the integral to calculate the vorticity distribution used for modeling this thin airfoil. So at the leading edge, γ will become infinite but regarding $\gamma \sin(\psi)$ as the fundamental variable this product remains finite at the leading edge and therefore causes no numerical difficulty. This means that the value of γ does not need to be considered at the trailing edge, but does at the leading edge. Therefore ψ can also be written as:

$$\psi = \frac{\pi l_1}{N} \;\; with : l_1 = 0, 1, 2, ..., (N-1) \tag{4.30}$$

It is convenient to choose ε - which is related to the points on the grid where the input velocities will be defined - such that these values lie midway between the values of ψ at which γ is specified:

$$\varepsilon = \frac{\pi(2l_2+1)}{2N} \;\; with : l_2 = 0, 1, 2, ..., (N-1) \tag{4.31}$$

It is supposed by Whitehead [21] that the upwash integral equation, using the definitions for ψ (equation 4.30) and ε (equation 4.31), can be evaluated by the trapezoidal rule. Whitehead states that approximating the upwash integral equation using the trapezoidal rule yields remarkably accurate results, although a correction is required for the logarithmic singularity in K if these accurate results are to be obtained with modest values of N [23]. In the paper of Whitehead [21] the Kernel function is treated such that it is redefined in terms of a modified Kernel function (which does not contain the troublesome logarithmic singularity) and a term describing the logarithmic singularity:

$$K(..) = K'(..) + K_{singularity} \tag{4.32}$$

Furthermore Whitehead evaluates this modified Kernel function in his Appendix III [21], where the end results is written down in equation (A13) in the paper of Whitehead. It is expected that Smith, although not written explicitly, uses this modified Kernel function such that the upwash integral equation becomes:

$$\begin{aligned} \sum_{l_1=0}^{N}{}' \left[\gamma \left(\frac{1-\cos\left(\frac{\pi l_1}{N}\right)}{2} \right) K' \left(\frac{\cos\left(\frac{\pi l_1}{N}\right) - \cos\left(\frac{\pi(2l_2+1)}{2N}\right)}{2} \right) \frac{\pi}{2N} \sin\left(\frac{\pi l_1}{N}\right) \right] \\ = -\bar{v}^{-}_{inc,m} \left(\frac{1-\cos\left(\frac{\pi(2l_2+1)}{2N}\right)}{2} \right) \end{aligned} \tag{4.33}$$

With $\sum_{l_1=0}^{N}{}'$ denoting a summation in which the first and last terms are given half weight (consequence of trapezoidal rule). It should be noted that the notation of Smith and Whitehead can be confusing, they use a vinculum to group $\overline{2l_2+1}$. It is confusing since this is a notation which is not used often in present days. This equation may be written in matrix-vector notation as:

$$[K]\underline{\Gamma} = \underline{v} \tag{4.34}$$

Where $[K]$ is a $N \times N$ matrix with the element in the l_2^{th} row and l_1^{th} column given by:

$$K' \left(\frac{\cos\left(\frac{\pi l_1}{N}\right) - \cos\left(\frac{\pi(2l_2+1)}{2N}\right)}{2} \right) \tag{4.35}$$

Again stated, this modified Kernel function is not defined in Smith and is not completely similar to the analytic Kernel function of equation (S31). It is the modified expression of this Kernel function, without the logarithmic singularity which is present in the analytic Kernel function. The vector $\underline{\Gamma}$ is a $N \times 1$ vector with the l_1^{th} entry given by:

$$\frac{\pi}{2N} \sin\left(\frac{\pi l_1}{N}\right) \gamma \left(\frac{1-\cos\left(\frac{\pi l_1}{N}\right)}{2} \right) \tag{4.36}$$

And $\underline{v}$ is also a $N \times 1$ vector with the l_2^{th} entry given by:

$$-\bar{v}^{-}_{inc,m} \left(\frac{1-\cos\left(\frac{\pi(2l_2+1)}{2N}\right)}{2} \right) \tag{4.37}$$

The direct solution of equation 4.34 is:

$$\underline{\Gamma} = [K]^{-1}\underline{v} \tag{4.38}$$

4.8 Numerical evaluation acoustic wave amplitudes

When $\underline{\Gamma}$ is calculated, the magnitudes of the transmitted and reflected transmitted pressure waves can be calculated using a numerical modification of equation 4.20. Once again, since it can be confusing, the difference in using r is explained. For calculating the vorticity distribution $\underline{\Gamma}$ using the upwash integral equation (equation 4.38), all pressure modes need to be considered ($r = -\infty...\infty$). However for calculating the magnitudes of the transmitted and reflected transmitted far field acoustic waves waves where the sub-resonance condition is satisfied: $r = 0$. In order to solve the integral in equation 4.20 numerically, again the trapezoidal rule is carried out for calculating the pressure wave amplitudes:

$$\hat{p}_m^{\pm} = -\frac{\rho_0 W}{s/c}(v')^{\pm}\frac{\left(\frac{\omega_0 c}{W}\right) + \mu_m^{\pm} c\cos(\alpha_s) + \nu_m c\sin(\alpha_s)}{\nu_m c} \sum_{l_1=0}^{n}{}' \left[\frac{\pi}{2n}\sin\left(\frac{\pi l_1}{N}\right)\gamma\right]\left[e^{-ic\bar{\mu}_m^{\pm}\left(\frac{1-\cos(\frac{\pi l_1}{N})}{2}\right)}\right] \tag{4.39}$$

With the magnitudes of the far field acoustic waves known, the transmission and reflection coefficients can be calculated using equation 3.39.

Chapter 5

Blade row model of Smith without mean stream flow

As already indicated in the previous chapter, the flow velocity cannot simply be set to zero in the model of Smith. This can be seen by setting W to zero in equation 4.13, the amplitudes - according to the model of Smith - will be infinite which is not physical. A couple of differences are summed here. The first difference can already be observed in the characteristic equation from the linearized equations of continuity and momentum (equation 4.2). When the fluid velocity is zero, there are no vorticity waves present. Only $\omega_0 = 0$ yields non-trivial solutions. Since there are no vorticity waves, the third boundary condition (a relation between the vorticity in the flow and the strength of the vorticity of the bound vortices placed on the blades) discussed in "4.4 Solution of one vortex row" cannot be used. This has the consequence that the amplitudes components for the transmitted and reflected waves ($v_m^{\pm}$ in equation 4.13) cannot be used from Smith. Finally this changes the Kernel function in the upwash integral equation (equation 4.19) and therefore the modified Kernel function of Whitehead [21] cannot be applied. Moreover, since the governing conservation equations are different, the ratios of the velocity and pressure amplitude components are different (equation 4.3). Therefore also the calculation of the total amplitude of the pressure wave (equation 4.20) is different. These differences indicate, that for a case without mean stream flow, the model needs to be 'build' from the same starting point as Smith carried out: the governing equations.

5.1 Governing equations

Again a pressure wave of a single circumferential wave number m originating far upstream impinging on a stator is considered, only now **without** mean flow. It is still assumed that the sub-resonant condition is satisfied ($k \leq \frac{\pi}{s}$). The linearized equations of continuity and momentum without mean stream flow read, assuming the medium is isentropic:

$$\begin{aligned} \frac{\partial p}{\partial t} + \rho_0 a^2 \left(\frac{\partial u}{\partial x} + \frac{\partial v}{\partial y} \right) &= 0 \\ \frac{\partial u}{\partial t} &= -\frac{1}{\rho_0} \frac{\partial p}{\partial x} \\ \frac{\partial v}{\partial t} &= -\frac{1}{\rho_0} \frac{\partial p}{\partial y} \end{aligned} \tag{5.1}$$

Also it is assumed the the perturbations are plane waves (equation 4.1). From these statements, the characteristic equation for non-trivial solutions of the conservation equation is found:

$$(\omega_0 + U\mu_{m,r}^{\pm} + V\nu_{m,r})^2 - a^2((\mu_{m,r}^{\pm})^2 + \nu_{m,r}^2) = 0 \tag{5.2}$$

When this is compared with the characteristic equation of the model of Smith with mean stream flow (equation 4.2), it is indeed observed that only pressure waves are present. The ratios of the amplitudes of the velocity and pressure components are similar as equation 4.3, but for the fact the mean stream flow is set to zero:

$$\begin{aligned} \frac{\hat{p}^{\pm}_{m,r}}{\hat{v}^{\pm}_{m,r}} &= -\frac{\omega_0 \rho_0}{\nu_{m,r}} \\ \frac{\hat{u}^{\pm}_{m,r}}{\hat{v}^{\pm}_{m,r}} &= \frac{\mu^{\pm}_{m,r}}{\nu_{m,r}} \end{aligned} \tag{5.3}$$

5.2 Incoming pressure wave

The calculation method for the incoming pressure wave is identical, since it is not directly linked to the method of Smith. However, since the ratios between the amplitudes of the velocity and pressure components are different, the incoming upwash velocity is a bit different. Applying the definition of the upwash velocity (equation 4.6), carrying out the coordinate transformation such that the $\bar{x}$-axis is placed along the blade chord and $\bar{y}$-axis normal to the blade chord (equation 4.8), using the convention of $\bar{\mu}^{\pm}_{m}$ and $\bar{\nu}^{\pm}_{m}$ of equation 4.10 and carry out the analysis on the reference blade ($\bar{y} = 0$) the upwash velocity for an arbitrary incoming pressure wave, propagating in downstream direction, without mean stream flow yields:

$$\bar{v}^{-}_{inc,m} = -\frac{\bar{\nu}^{-}_{inc,m}}{\omega_0 \rho_0} \hat{p}_{inc,m} e^{i\left(\omega_0 t + \bar{\mu}^{-}_{inc,m} \bar{x}\right)} \tag{5.4}$$

5.3 Solution of one vortex row

Next step in the method of Smith is to find the solution of one vortex row of the blade row. The boundary conditions used in Smith's paper cannot be used similarly. As already indicated, the condition that there is no net upwash at the blade surface should be satisfied (since no air can flow through the blades). For the sake of clarity the axial and gap-wise velocity components in the (x,y) reference frame are derived using the ratios between the amplitudes of the velocity and pressure components 5.3. Note that these are velocity perturbations produced by the vortices. Already discussed in the previous chapter, although for the far field acoustic waves only a specific part of pressure modes are present, all modes are effecting the near field:

$$\begin{aligned} u^{\pm}_{m,r} &= -\frac{\mu^{\pm}_{m,r}}{\omega_0 \rho_0} \hat{p}^{\pm}_{m,r} e^{i(\omega_0 t + \mu^{\pm}_{m,r} x + \nu_{m,r} y)} \\ v^{\pm}_{m,r} &= -\frac{\nu_{m,r}}{\omega_0 \rho_0} \hat{p}^{\pm}_{m,r} e^{i(\omega_0 t + \mu^{\pm}_{m,r} x + \nu_{m,r} y)} \end{aligned} \tag{5.5}$$

First condition applied on the velocity perturbations produced by these vortices is the equation of continuity through the cascade. The vortices produce up- and downstream pressure waves. Therefore in order to satisfy the equation of continuity, the magnitudes of the axial velocity perturbations at the cascade should be equal:

$$\frac{\mu^{+}_{m,r}}{\omega_0 \rho_0} \hat{p}^{+}_{m,r} - \frac{\mu^{-}_{m,r}}{\omega_0 \rho_0} \hat{p}^{-}_{m,r} = 0 \tag{5.6}$$

From the relation of the axial wave number (equation 3.9), setting the Mach numbers to zero, it is found that:

$$\mu^{+}_{m,r} = -\mu^{-}_{m,r} \tag{5.7}$$

Plugging this into equation 5.6:

$$\hat{p}^{+}_{m,r} + \hat{p}^{-}_{m,r} = 0 \tag{5.8}$$

The second condition comes from the velocity jump in y-direction as the cascade is crossed. This velocity jump should be similar to the strength of the vortices on blades (Γ):

$$\hat{p}^{+}_{m,r} - \hat{p}^{-}_{m,r} = \frac{\omega_0 \rho_0}{\nu_{m,r}} \frac{\Gamma}{s} \tag{5.9}$$

Equation 5.8 and 5.9 yield the magnitude of the transmitted (-) and reflected (+) pressure waves:

$$\hat{p}^{\pm} = \pm \frac{\omega_0 \rho_0}{2\nu_{m,r}} \frac{\Gamma}{s} \tag{5.10}$$

The magnitudes of the transmitted and reflected pressure waves now also depend on the strength of the vorticity and the blade gap. Substituting this into equation 4.1 yields the relations for the transmitted and reflected pressure waves. In terms of the reference frame along the chord ($\bar{x}$,$\bar{y}$) and applied on the reference blade ($\bar{y}$=0) this reads:

$$p^{\pm}_{m,r}(\bar{x}, t) = \pm \frac{\Gamma}{s} \frac{\omega_0 \rho_0}{2\nu_{m,r}} e^{i\left(\omega_0 t + \bar{\mu}^{\pm}_{m,r} \bar{x}\right)} \tag{5.11}$$

5.4 Upwash integral equation

For the derivation of the upwash integral equation the similar approach as in the previous chapter (and therefore similar to the method of Smith) is carried out. Using the ratio between the pressure amplitude and the gap-wise velocity amplitude (equation 5.3) the induced upwash velocities at the point $\bar{x}$ on the reference blade is found:

$$\bar{v}^{\pm}_{m,r}(\bar{x}) = \pm \frac{1}{2} \frac{\gamma(\bar{x}_0) d\bar{x}_0}{s} \sum_{r=-\infty}^{\infty} e^{i(\omega_0 t + \bar{\mu}^{\pm}_{m,r}(\bar{x} - \bar{x}_0))} \tag{5.12}$$

The relevant velocities for $(\bar{x} - \bar{x}_0) < 0$ are those associated with the upstream pressure perturbation (+); for $(\bar{x} - \bar{x}_0) > 0$ those associated with the downstream pressure perturbation (-). The total upwash induced by the cascade is found by integration along the blade chord:

$$\begin{aligned} \bar{v}^{\pm}_{m,r}(\bar{x}) = &- \int_0^{\bar{x}} \frac{\gamma(\bar{x}_0)}{2s} \sum_{r=-\infty}^{\infty} e^{i(\omega_0 t + \bar{\mu}^{-}_{m,r}(\bar{x} - \bar{x}_0))} d\bar{x}_0 \\ &- \int_{\bar{x}}^{c} \frac{\gamma(\bar{x}_0)}{2s} \sum_{r=-\infty}^{\infty} e^{i(\omega_0 t + \bar{\mu}^{+}_{m,r}(\bar{x} - \bar{x}_0))} d\bar{x}_0 \end{aligned} \tag{5.13}$$

This relation can be rewritten using a convenient coordinate transformation $\tilde{x} = \frac{1}{c}\bar{x}$ in order to obtain a dimensionless interval for the integral. Also here the summation of the upwash velocity corresponding to the bound vortices and the incoming pressure waves, respectively, should be zero. Applying this leads to:

$$\begin{aligned} -\bar{v}^{\pm}_{inc,m}(\tilde{x}) &= \int_0^1 \gamma(\tilde{x}_0) K(\tilde{x} - \tilde{x}_0) d\tilde{x}_0 \\ &with: K(\eta) = -\frac{1}{(2s/c)} \sum_{r=-\infty}^{\infty} e^{i(\omega_0 t + c\bar{\mu}^{-}_{m,r}\eta)} \; for\, \eta > 0 \\ &and: K(\eta) = -\frac{1}{(2s/c)} \sum_{r=-\infty}^{\infty} e^{i(\omega_0 t + c\bar{\mu}^{+}_{m,r}\eta)} \; for\, \eta < 0 \end{aligned} \tag{5.14}$$

Which is a similar looking equation as the upwash integral equation for the method of Smith with free stream flow (equation 4.19). However be aware that the Kernel function is different for the two cases.

5.5 Far field acoustic waves

Solving the upwash integral equation yields the vorticity distribution, which is used to calculate the magnitudes of the far field acoustic waves. This is carried out using equation 5.11 and the definition of the plane wave (equation 4.1) for which should be observed that each chordal element of the cascade forms a vortex row contributing to the magnitudes of the waves:

$$\begin{aligned} \hat{p}^{\pm}_{m,r} &= \pm \frac{\omega_0 \rho_0}{2\nu_{m,r}} \frac{\Gamma}{s} e^{-i\bar{\mu}^{\pm}_{m,r}\bar{x}_0} \\ &= \pm \frac{\omega_0 \rho_0}{\nu_{m,r}(2s/c)} \int_0^1 \gamma(\tilde{x}_0) e^{-i\tilde{\mu}^{\pm}_{m,r}\tilde{x}_0} d\tilde{x}_0 \end{aligned} \tag{5.15}$$

Which is again quite similar equation 4.20, but for differences concerning the absence of mean stream velocity.

5.6 Numerical evaluation upwash integral equation and acoustic wave amplitudes

The same collocation technique is carried out to solve the upwash integral equation. Carrying out the coordinate transformation of equation 4.21 on the upwash integral equation (equation 5.14), setting ψ and ε following equations 4.30 and 4.31 and applying the trapezoidal rule yields:

$$\begin{aligned} &\sum_{l_1=0}^{n}{}' \left[\gamma\left(\frac{1-\cos\left(\frac{\pi l_1}{n}\right)}{2} \right) K'\left(\frac{\cos\left(\frac{\pi l_1}{n}\right) - \cos\left(\frac{\pi(2l_2+1)}{2n}\right)}{2} \right) \frac{\pi}{2n} \sin\left(\frac{\pi l_1}{n}\right) \right] \\ &\quad = -\bar{v}^{-}_{inc,m} \left(\frac{1-\cos\left(\frac{\pi(2l_2+1)}{2n}\right)}{2} \right) \end{aligned} \tag{5.16}$$

Similar as equation 4.34, this may be written in matrix-vector notation:

$$[K]\underline{\Gamma} = \underline{v} \tag{5.17}$$

With the direct solution:

$$\underline{\Gamma} = [K]^{-1}\underline{v} \tag{5.18}$$

In the original paper of Smith, the Kernel function is corrected such that accurate results are to be obtained with modest values of N. One can try to carry out a similar correction by finding a modified Kernel function for the case without mean stream flow by investigating the calculation method of Whitehead carefully. However, it is stated in a review article of Whitehead in 1987 [23] that this correction of the Kernel is required such that accurate results with modest values of N is obtained. This also suggest that the Kernel function (including the logarithmic singularity) should yield accurate results for large values of N and therefore in principle can be solved using equation 5.18.

With the vorticity distribution obtained, the magnitudes of the far field acoustic waves can be calculated using the numerical modification of equation 5.15:

$$\hat{p}^{\pm}_{m,r} = \pm \frac{\omega_0 \rho_0}{\nu_{m,r}(2s/c)} \sum_{l_1=0}^{n}{}' \left[\frac{\pi}{2n} \sin\left(\frac{\pi l_1}{n}\right) \gamma \right] \left[e^{-ic\bar{\mu}^{\pm}_{m,r}\left(\frac{1-\cos(\frac{\pi l_1}{n})}{2}\right)} \right] \tag{5.19}$$

The transmission and reflection coefficients are obtained by applying the results of this procedure (the amplitudes of the transmitted and reflected power waves) in the relations for the coefficient (equation 3.39).

Chapter 6

Results

In this chapter the preliminary results of the original model of Smith - with mean stream flow - is discussed. In order to enhance the readability of this chapter, the course of events is explained. In the time available, it was first attempted to carry out calculations for the modified model of Smith, since experiments without mean stream flow are planned at DLR. However, the results using an implemented calculation program with MATLAB did not yield satisfactory results. Therefore it is thought to duplicate the calculations carried out by Smith, such that the validity of the calculation program can be investigated and to give more insight in the possible unforeseen difficulties arising when the theoretical model is implemented. In this chapter typical results of the blade row models of the 1970's (see literature review in chapter 2) is presented, the implemented MATLAB program is explained and the raw results are discussed. Since the results of the duplicated model of Smith do not yield satisfactory results, it cannot be expected to find accurate results for the model without mean stream flow. Therefore only the results of the current program which calculates the transmission and reflection coefficients following the original model of Smith are presented and discussed in this report.

6.1 Typical results of blade row models

As is indicated in the literature review, Kaji and Okazaki were the pioneers examining the subject of the transmission of sound waves through blade rows. The blade row models defined after Kaji and Okazaki in the 1970's (Smith, Koch, Amiet, a.o.) presented the transmission and reflection coefficients such that they can compare their results with the results of Kaji and Okazaki. The results of the transmission and reflection coefficients from Smith are visualized in figure 6.1. The results from Smith are for an upstream propagating incident wave with $s/c = 1$, the blade stagger angle of 60^o, the flow Mach number 0.5 and an in Smith defined frequency parameter $\lambda = \pi/2$. The black lines present the results of Kaji and Okazaki [4], the open and closed circles represent the transmission and reflection coefficients from the calculation method of Smith. Since similar parameters are used, it is expected that the calculation program, implementing the original method of Smith yields similar results as displayed in figure 6.1.

6.2 Implementation in MATLAB

The model of Smith is implemented in MATLAB using three files: 'Main upstream', 'Kernel whitehead' and 'V whitehead'. The main file contains most implementation of the model of Smith, the file containing the Kernel function calculates every index for the modified Kernel matrix (equation 4.35) in which the function V from the paper of Whitehead [21] is applied. These files can be found in Appendix B. Here an overview of the MATLAB program is given:

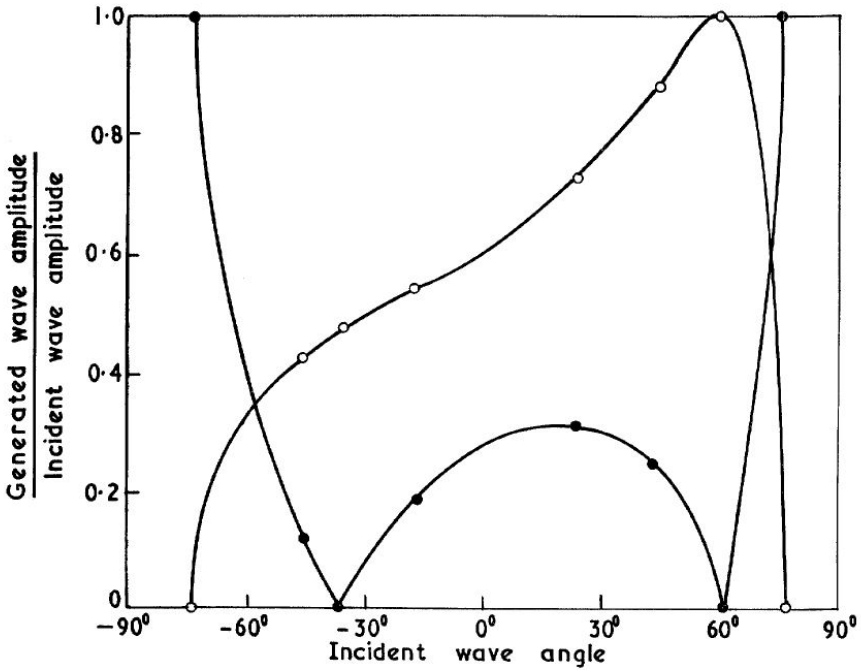

Figure 6.1: Results from Smith [1]

Input:
In this section the input parameters are defined such as the geometry of the blades, the mean stream velocity and the frequency of the pressure waves.
Grid:
The number of grid points N is defined. This also resembles the number of vortices placed on the blades. Smith finds accurate results between $N = 4$ and $N = 10$.
Incoming pressure wave:
The parameters of the incoming pressure waves are defined and calculated such as the circumferential wave number m, the amplitude of the wave, the wave numbers, the input upwash velocity vector and the angle of incidence.
Kernel function:
The inter-vane phase difference is calculated and the Kernel matrix is formed. This is based on the modified Kernel function of Whitehead K'. Using the Kernel matrix and the incoming upwash velocity vector the vorticity distribution is calculated.
Magnitude of far acoustic field:
Following the method of Smith the amplitudes of the far field acoustic waves are calculated.
Transmission and Reflection:
Based on equation 3.39 the transmission and reflection coefficients are calculated.

6.3 Raw results

As already mentioned a couple of times, the implementation of the model of Smith is not finished. The results from current calculation program (Appendix B) yield results which do not match the results of Smith. As can be seen in figure 6.1 the expected transmitted and reflected coefficient by incident angle 0^o for the similar parameters used in Smith are:

$$\begin{aligned} \mathcal{T}_{m,Smith} &\approx 0.59 \\ \mathcal{R}_{m,Smith} &\approx 0.29 \end{aligned} \tag{6.1}$$

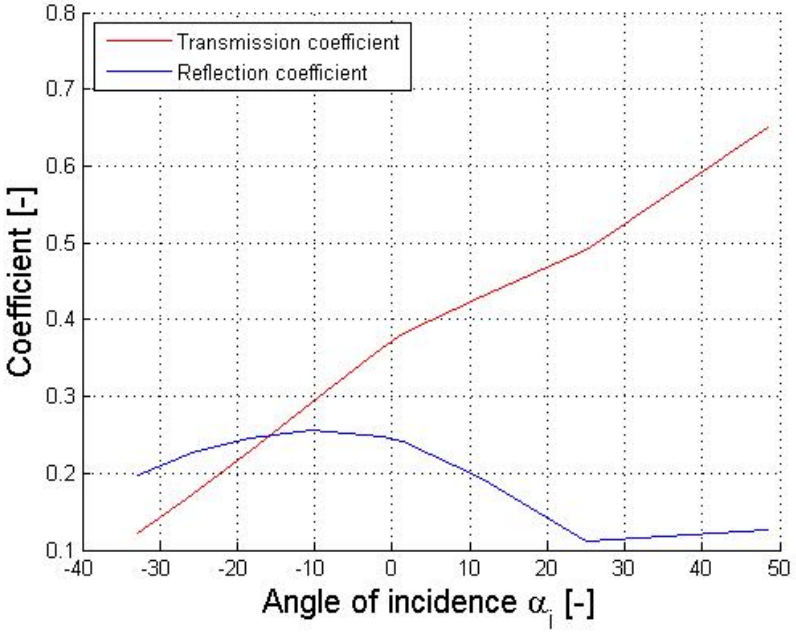

Figure 6.2: Results of current program

The results from current calculation program are:

$$\begin{aligned} \mathcal{T}_{m,current} &\approx 0.37 \\ \mathcal{R}_{m,current} &\approx 0.23 \end{aligned} \tag{6.2}$$

In figure 6.2 the results from current program for multiple angles of incidence is found. It can be seen directly these results do not match the results of Smith 6.1. This means there are still flaws present; either in the theory, in the implementation of the theory, or both. It is not understood what causes these deviations with the results of Smith. One specific detail is mentioned; it seems that a zero incidence angle is not suitable for calculating the transmission and reflection coefficients. If the angle of incidence is zero, the gap-wise wave number $\nu_{m,inc}$ is zero, from which follows that the inter-vane phase difference σ_m is zero. This indicates that, for far field acoustic waves, the gap-wise wave number for the transmitted and reflected waves are zero. And this has the consequence that the amplitudes of the y-velocity components of the acoustic waves is infinite (since in the definition of Smith there is a term $1/\nu_m$). This is of course not physical. This can mean two things, or indeed the model of Smith is not applicable for cases with the angle of incidence being equal to zero (which Smith did not mentions in his paper), or this is a clue to the error in the implementation of the model or the inter-vane phase difference.

Chapter 7

Conclusion

7.1 Main conclusions

The first objective of the present study was to carry out a review of literature regarding existing analytical models that describe the propagation of sounds waves through turbomachinery blade rows. From this analysis it is found that analytical models are defined in the 1970's with Kaji Okazaki [5], [4] as pioneers in this field. Two models (Smith [1] and Koch [7]) are used often in literature after the 1970's, both using different mathematical tools to describe the sound waves through blade rows. Also other phenomena, such as mode trapping and acoustic resonance are discussed in literature. These effect should be considered when calculation models for multiple blade rows are defined.

The theory of the blade row model of Smith is discussed in chapter 4, from which it is found that the paper of Smith can only be understood correctly with knowledge of the model of Whitehead [21]. A modification of Smith's blade row model is presented in chapter 5, which is supposed to be theoretically valid. The implementation of the original and the modified model of Smith is not complete, there are still flaws in the understanding of the theory, the implementation of the model, or both. However, since Smith presents results in his paper, it is believed that the understanding of the theory and/or the implementation of the model is achievable. It should also be noted, since the implementation of the modified model is lacking, the validity of the theoretical modification of the blade row model of Smith is not checked. When applying the modified model, one should be aware of this fact.

7.2 Recommendations

The most significant development that needs to be carried out is to find the errors in the current calculation program. The only hint, which is also discussed in the results, of a possible error is the disability of the current program to cope with a zero incidence angle. More examination of the model in Smith for deeper understanding and better implementation is therefore recommended. When the calculation program for the original model of Smith is valid, the attention can shift towards implementation of the modified model of Smith. The results from the modified model are recommended to use for examining the validity of the theoretical modification of the blade row model.

If the calculation program for the modified blade row model is operational, experiments can be conducted for sound waves propagating through ducted turbomachinery blade rows. It is advised to investigate the comparisons and differences between the results from the (modified) model of Smith and experiments. Future research should enhance the understanding of sound waves propagating through blade rows, which can be applied in other studies, for example in

studies on noise reduction for airplane engines.

Bibliography

[1] S. Smith, "Discrete frequency sound generation in axial flow turbomachines," *Aeronautical Research Council Reports and Memoranda*, 1972.

[2] S. Glegg, "The response of a swept blade row to a three-dimensional gust," *Journal of sound and vibration*, vol. 227, no. 1, pp. 29–64, 1999.

[3] R. Muir, "The application of a semi-actuator disk model to sound transmission calculations in turbomachinery, part i: The single blade row," *Journal of Sound and Vibration*, vol. 54, no. 3, pp. 393–408, 1977.

[4] S. Kaji and T. Okazaki, "Propagation of sound waves through a blade row: Ii. analysis based on the acceleration potential method," *Journal of Sound and Vibration*, vol. 11, no. 3, pp. 355 – IN1, 1970.

[5] S. Kaji and T. Okazaki, "Propagation of sound waves through a blade row: I. analysis based on the semi-actuator disk theory," *Journal of Sound and Vibration*, vol. 11, no. 3, pp. 339 – 353, 1970.

[6] R. Mani and G. Horvay, "Sound transmission through blade rows," *Journal of sound and vibration*, vol. 12, no. 1, pp. 59–83, 1970.

[7] W. Koch, "On the transmission of sound waves through a blade row," *Journal of sound and vibration*, vol. 18, no. 1, pp. 111–128, 1971.

[8] R. Amiet, "Transmission and reflection of sound by a blade row," *AIAA Journal*, vol. 9, no. 10, pp. 1893–1894, 1971.

[9] D. Topol, S. Holhubner, and D. Mathews, "A reflection mechanism for aft fan tone noise from turbofan engines," in *American Institute of Aeronautics and Astronautics Conference*, vol. 1, 1987.

[10] J. M. Tyler and T. G. Sofrin, "Axial flow compressor noise studies," tech. rep., SAE Technical Paper, 1962.

[11] D. Hanson, "Mode trapping in coupled 2d cascades-acoustic and aerodynamic results," *AIAA Paper*, no. 93-4417, 1993.

[12] D. B. Hanson, "Acoustic reflection and transmission of 2-dimensional rotors and stators, including mode and frequency scattering effects," *AIAA Paper*, 1999.

[13] D. B. Hanson, "Broadband noise of fans-with unsteady coupling theory to account for rotor and stator reflection/transmission effects," *Contractor report NASA*, no. 2001-210762, 2001.

[14] H. Posson, H. Bériot, and S. Moreau, "On the use of an analytical cascade response function to predict sound transmission through an annular cascade," *Journal of Sound and Vibration*, vol. 332, no. 15, pp. 3706–3739, 2013.

[15] D. A. Topol, "Development and evaluation of a coupled fan noise design system," *AIAA Paper*, no. 97-1611, 1997.

[16] P. D. Silkowski and K. C. Hall, "1997 best paper award - structures and dynamics committee: A coupled mode analysis of unsteady multistage flows in turbomachinery," *Journal of turbomachinery*, vol. 120, no. 3, pp. 410–421, 1998.

[17] R. Parker, "Acoustic resonances and blade vibration in axial flow compressors," *Journal of Sound and Vibration*, vol. 92, no. 4, pp. 529–539, 1984.

[18] B. Hellmich and J. R. Seume, "Causes of acoustic resonance in a high-speed axial compressor," *Journal of Turbomachinery*, vol. 130, no. 3, 2008.

[19] W. Neise and U. Michel, *Aerodynamics Noise of Turbomachines*. DLR Internal Report 22314-94/B5, Institute of Propulsion Technology, Department of Engine Acoustics, 1994.

[20] G. Jenkins, *Models for the prediction of rear-arc and forward-arc fan broadband noise in turbofan engines*. PhD thesis, University of Southampton, 2013.

[21] D. S. Whitehead, *Force and moment coefficients for vibrating aerofoils in cascade*. HM Stationery Office, 1962.

[22] J. Anderson, *Fundamentals of Aerodynamics*. McGraw-Hill Series in Aeronautical and, McGraw-Hill Higher Education, 4 ed., 2007.

[23] D. Whitehead, "Classical two-dimensional methods," *In AGARD Aeroelasticity in Axial-Flow Turbomachines.*, vol. 1, 1987.

[24] A. Fritzsch, "Numerische untersuchung der transmission, reflexion und streuung von schallwellen an einem schaufelgitter," Master's thesis, Technische Universität Berlin, Institut für Strömungsmechanik und Technische Akustik, 2009.

Appendix A

Power coefficients

The second definition is the ratio of the acoustic powers of the transmitted, reflected and incoming sound waves, for example used in Hanson [11], [12]. A measure of the energy of sound per time unit is called the acoustic or sound power. This acoustic power is defined as the sound intensity (sound power per area) times the corresponding area. For a circular duct, unwrapped into the two-dimensional reference frame, it reads:

$$\mathcal{P}^{\pm} = \int_0^{2\pi} I_x^{\pm} R_0 d\phi = \int_0^{Bs} I_x^{\pm} dy \tag{A.1}$$

With I_x the sound intensity in axial direction. The intensity is not really integrated over a surface, but over a line. This power can therefore also be interpreted as a power density of the sound. The sound intensity for a pressure wave with zero mean flow is defined as [24]:

$$I_x^{\pm} = \frac{1}{2}\Re(p^* u) \tag{A.2}$$

$$= \left|\frac{1}{2}(p_{re}u_{re} + p_{im}u_{im})\right| \tag{A.3}$$

With subscript re stating the real part and the imaginary part is noted with subscript im. The velocity perturbations can be obtained applying the linearized x-momentum equation for zero mean flow, here carried out for the transmitted and reflected pressure waves from a stator when the sub-resonance condition 3.12 is satisfied. Note however that the same analysis can also be carried out for rotors and for super-resonance conditions:

$$\frac{\partial u}{\partial t} = -\frac{1}{\rho_0}\frac{\partial p}{\partial x} \tag{A.4}$$

With the mean density of the medium ρ_0. Using this relation, the axial velocity perturbation is found:

$$u_m^{\pm} = -\frac{\mu_m^{\pm}}{\omega_0 \rho_0} \hat{p}_m^{\pm} e^{i(\omega_0 t + \mu_m^{\pm} x + \nu_m y)} \tag{A.5}$$

With this the pressure and velocity perturbations are known, these are plugged into the definition of the axial intensity (equation A.3), which is then substituted into the equation for the acoustic power (equation A.1):

$$\mathcal{P}^{\pm} = \int_0^{Bs} \left|\frac{1}{2}\frac{\mu_m^{\pm}}{\omega_0 \rho_o}(\hat{p}_m^{\pm})^2\right| dy \tag{A.6}$$

$$= \left|\frac{1}{2}\frac{\mu_m^{\pm} Bs}{\omega_0 \rho_o}(\hat{p}_m^{\pm})^2\right| \tag{A.7}$$

Similar procedure can be carried out for the incoming pressure wave. This yields:

$$\mathcal{P}_{inc} = \left| \frac{\mu^{-}_{inc,m} Bs}{\omega_0 \rho_o} (\hat{p}_{inc,m})^2 \right| \tag{A.8}$$

The transmission and reflection coefficients are ratios of the transmitted/reflected acoustic power and the incoming acoustic power [11]. Using this definition, the transmission coefficient for the pressure wave modes impinging on a stator with zero mean flow is:

$$\mathcal{T}_m = \frac{\mathcal{P}^{-}}{\mathcal{P}_{inc}} = \left| \frac{\mu^{-}_{m} (\hat{p}^{-}_{m})^2}{\mu^{-}_{inc,m} (\hat{p}_{inc,m})^2} \right| \tag{A.9}$$

And the reflection coefficient:

$$\mathcal{R}_m = \frac{\mathcal{P}^{+}}{\mathcal{P}_{inc}} = \left| \frac{\mu^{+}_{m} (\hat{p}^{+}_{m})^2}{\mu^{-}_{inc,m} (\hat{p}_{inc,m})^2} \right| \tag{A.10}$$

The relation for the reflection coefficient can be rewritten into a representation from which the validity of both relations (transmission and reflection) can be verified. This is done by noting that the acoustic power of the incoming pressure wave and the transmitted and reflected pressure waves are related to each other. Assuming that the blade row does not produce or dissipates energy, the acoustic power of the incoming pressure wave should equal the sum of the acoustic power of the transmitted and reflected pressure waves:

$$\mathcal{P}_{inc} = \mathcal{P}^{-} + \mathcal{P}^{+} \tag{A.11}$$

Substituting the expressions for the acoustic power (equation A.8 and A.7) yields:

$$\left| \mu^{-}_{inc,m} (\hat{p}_{inc,m})^2 \right| = \left| \mu^{-}_{m} (\hat{p}^{-}_{m})^2 \right| + \left| \mu^{+}_{m} (\hat{p}^{+}_{m})^2 \right| \tag{A.12}$$

Substituting then this equation (A.12) into the relation for the reflection coefficient (equation A.10) gives:

$$\mathcal{R}_m = \left| \frac{\mu^{+}_{m} (\hat{p}^{+}_{m})^2}{\mu^{-}_{inc,m} (\hat{p}_{inc,m})^2} \right| = \left| \frac{\mu^{-}_{inc,m} (\hat{p}_{inc,m})^2 - \mu^{-}_{m} (\hat{p}^{-}_{m})^2}{\mu^{-}_{inc,m} (\hat{p}_{inc,m})^2} \right| = 1 - \mathcal{T}_m \tag{A.13}$$

So for the case of total transmission (all of the acoustic power of the incoming pressure wave transmits through the blade row), the transmission coefficient $\mathcal{T}_m$ is one, implying that the reflection coefficient $\mathcal{R}_m$ is zero, which fulfills the expectation.

Appendix B

MATLAB scripts

B.1 Main upstream

```
close all
clear all
clc

%% Input Parameters

B = 25 ;              % [-]       Number of blades of stator
R = 0.25 ;            % [m]       Radius of blades
s = 2*pi*R/B ;        % [m]       Blade Gap
c = s;                % [m]       Blade Chord

Um = 85;              % [m/s]     Axial Free stream velocity
Vm = Um*1.73;         % [m/s]     Gap-Wise Free stream velocity
W = sqrt(Um^2+Vm^2);% [m/s]     Mean stream flow
a = 343 ;             % [m/s]     Speed of sound
M = W/a ;             % [-]       Mach Number

as = atan(Vm/Um) ;    % [rad]     Stagger angle

w = 2*pi*675;         % [rad/s]   Acoustic frequency
rho = 1.2 ;           % [kg/m^3]  Density of fluid

l = w*c/W ;           % [-]       Frequency parameter
wl = 2*pi*a/w;        % [m]       Wave length

k = w/a ;             % [-]       Wave number

%% Display

disp('----Sub-Resonance?----------------------')

if (k)<=(pi/s*(1-M^2)/sqrt(1-M^2*cos(as)^2))
    fprintf('yes! \n')
    fprintf('%.2f (w/a) <= %.2f (pi/s*(1-M^2)/sqrt(1-M^2*cos(as)^2))\n \n'
        ,w/a,pi/s*(1-M^2)/sqrt(1-M^2*cos(as)^2))
end
disp('----Compare with Smith:-------')
fprintf('as  = %.0f     (stagger angle)\n',as*180/pi)
fprintf('s/c = %.2f     (gap/chord)\n',s/c)
fprintf('M   = %.2f     (Mach Number)\n',M)
```

```
41 fprintf('l    = %.2f      (Frequency parameter)\n',l)
42 fprintf('wl   = %.2f      (Wave Length)\n',wl)
43 fprintf('wl/c= %.2f      (Wave Length/chord)\n',wl/c)
44
45 %% Grid
46 n = 10 ;                 % Number of grid points
47 range =  0:(n-1) ;
48
49 fprintf('n    = %.0f      (Number of grid points)\n',n)
50
51 %% Incoming acoustic wave
52
53 m = 0.01 ;               % [-]       Circumferential wave number
54 P_inc = 1 ;              % [N/m^2]   Magnitude of incoming acoustic wave
55
56 fprintf('m    = %1.f      (circumferential mode order)\n',m)
57
58 % Incoming acoustic field
59 nu_inc = 2*pi*m/(B*s) ;      % Gap wise wave number
60 f1 = w+Vm*nu_inc ;           % component in axial wave number
61 f2 = a^2-Um^2 ;              % component in axial wave number
62 mu_inc = (Um*f1+a*sqrt(f1^2-f2*nu_inc^2))/f2 ;  % Axial wave number
63
64 if imag(mu_inc) ~= 0
65     display('----------------------------------------')
66     display('Error: Incoming pressure wave is cut-off!')
67     display('----------------------------------------')
68 end
69
70 % Calculating the incoming upwash velocity vector
71 range2 = range(:) ;
72 eta = (1-cos(pi*(2*range2+1)/(2*n)))/2 ;
73
74 f1 = P_inc/((w+Um*mu_inc+Vm*nu_inc)*rho) ;
75 f2 = mu_inc*sin(as)-nu_inc*cos(as) ;
76 f3 = 1i*c*eta*(mu_inc*cos(as)+nu_inc*sin(as)) ;
77 V =  -f1*f2*exp(f3) ;
78
79 aw = atan(-nu_inc/mu_inc) ;
80 fprintf('aw   = %.0f    (Incident wave angle)\n\n',aw*180/pi)
81
82 %% Kernel Function
83
84 % Inter-vane-phase-difference
85 sigma =  nu_inc*s;
86
87 % Input for the Kernel Function (whitehead)
88 ak = c/s*cos(as) ;
89 bk = c/s*sin(as) ;
90
91 K = zeros(n,n) ;
92
93 % Calculating the terms of Kernel Matrix
94 for l2 = range
95     for l1 = range
96         eta = 1/2*(cos(pi*l1/n)-cos(pi*(2*l2+1)/(2*n))) ;
97         K(l2+1,l1+1)=Kernel_whitehead(eta,l,sigma,ak,bk,n,l1) ;
98     end
99 end
100
```

```
%% Upwash Integral equation

% Taking half of the value of the first terms, because of usage
% of Trapazoidal rule
K(:,1) = K(:,1)/2 ;

% Calculation of the Vorticity vector. Note that by using trapezoidal
% rule that the values of first and last terms are already half weighted.
T = K\V ;

%% Magnitude of far field acoustic waves (r=0)

% Parameters for acoustic waves
r = 0;                          % No mode scattering
nu = (sigma-2*pi*r)/s ;         % y-wave number for transmitted waves
A = l^2+(nu*c)^2+2*l*(nu*c)*sin(as);    % Factor

eta = (1-cos(pi*range/n))/2 ;

% axial wave numbers
% p(plus) = reflected, m(min) = transmitted
f1 = w+Vm*nu ;
f2 = a^2-Um^2 ;
mu1 = (Um*f1+a*sqrt(f1^2-f2*nu^2))/f2 ;
mu2 = (Um*f1-a*sqrt(f1^2-f2*nu^2))/f2 ;

% Amplitudes of y-velocity components
f1 = (nu*c)^2/(2*A) ;
f2 = (1i*l*cos(as))/sqrt((nu*c)^2-M^2*A) ;
v1 = f1*(-1-l/(nu*c)*sin(as)+f2) ; % nu-hat instead of nu
v2 = f1*(1+l/(nu*c)*sin(as)+f2) ;

% Function V from smith
f1 = (l+c*mu1*cos(as)+c*nu*sin(as))/(nu*c) ;
f2 = -1i*c*eta*(mu1*cos(as)+nu*sin(as)) ;
Vs1 = -1/(s/c)*v1*f1*exp(f2) ;

f1 = (l+c*mu2*cos(as)+c*nu*sin(as))/(nu*c) ;
f2 = -1i*c*eta*(mu2*cos(as)+nu*sin(as)) ;
Vs2 = -1/(s/c)*v2*f1*exp(f2) ;

% Taking half of the value of the first terms, because of usage
% of Trapazoidal rule
Vs1(1) = 1/2*Vs1(1) ;
Vs2(1) = 1/2*Vs2(1) ;

% Calculating Magnitudes of far field acoustic waves
P1 = rho*W*dot(T,Vs1) ;
P2 = rho*W*dot(T,Vs2) ;

%% Transmission and reflection

% Transmission coefficient
Trans = (abs(P1)/P_inc) ;
% Reflection coefficient
Refl = (abs(P2)/P_inc) ;

disp('___Results of program:____')
fprintf('Transmission = %.2f \n',Trans)
fprintf('Reflection   = %.2f \n',Refl)
```

B.2 Kernel whitehead

```
function [ K ] = Kernel_whitehead(eta,l,sigma,a,b,n,l1)
%Kernel Function

% From sigma to beta:
beta = sigma ;
while beta < 0
    beta = beta + 2*pi ;
end
while beta >= (2*pi)
    beta = beta - 2*pi ;
end

% Function V from whitehead. First term in K' function.
V_func = V_whitehead(eta,beta,a,b) ;

% Second term in K' function, the integral:
z = -eta ;

range1 = linspace(z,1,10001);
if any(range1==0)
    display('Error: 0-value in the range')
end
F1 = 0 ;
counter = 0 ;
for z_hat = range1
    counter = counter + 1 ;
    f1 = exp(-1i*l*z_hat)*V_whitehead(-z_hat,beta,a,b) ;
    if (counter == 1) || (counter == length(range1))
        F1 = F1 + (f1 + 1/(2*pi*z_hat))/2;
    else
        F1 = F1 + f1 + 1/(2*pi*z_hat);
    end
end
F1 = F1*(1-z)/length(range1) ;

% Third term in K' function, the summations:
range2 = 0:100 ;

F2 = 0 ;
F3 = 0 ;
for r = range2
    f1 = exp(-(2*pi*r+beta)*(a+1i*b)-1i*l) ;
    f2 = (2*pi*r+beta)+1i*l/(a+1i*b) ;
    F2 = F2 + f1/f2 ;
    if r ~= 0
        f3 = exp(-(2*pi*r-beta)*(a-1i*b)-1i*l) ;
        f4 = (2*pi*r-beta)+1i*l/(a-1i*b) ;
        F3 = F3 + f3/f4 ;
    end
end

K = V_func-1i*l*exp(1i*l*z)*(F1-1/2*F2-1/2*F3) ;
end
```

B.3 V whitehead

```
function [ V ] = V_whitehead(eta,beta,a,b)

if beta == 0
    f1 = 1/4*(a+1i*b)*coth(pi*eta*(a+1i*b)) ;
    f2 = 1/4*(a-1i*b)*coth(pi*eta*(a-1i*b)) ;
    V = f1 + f2 ;
else
    f1 = 1/4*(a+1i*b)*exp(-(pi-beta)*(a+1i*b)*eta)/sinh(pi*(a+1i*b)*eta) ;
    f2 = 1/4*(a-1i*b)*exp((pi-beta)*(a-1i*b)*eta)/sinh(pi*(a-1i*b)*eta) ;
    V = f1 + f2 ;
end

end
```